CONTINUUM FLOW MODELS

BY REINHART KUHNE[7]
PANOS MICHALOPOULOS[8]

[7] Managing Director, Steierwald Schonharting und Partner, Hessbrühlstr. 21c 70565 Stuttgart, Germany

[8] Professor, Department of Civil Engineering, University of Minnesota Institute of Technology, 122 Civil Engineering Building, 500 Pillsbury Drive S.E., Minneapolis, MN 55455-0220

CHAPTER 5 - Frequently used Symbols

a	=	dimensionless traffic parameter
A	=	stop-start wave amplitude
α	=	sensitivity coefficient
b	=	net queue length at traffic signal
c	=	$g + r$ = cycle length
c_{0_2}	=	coefficient
c_0^2	=	constant, independent of density k
ds	=	infinitesimal time
Δt, Δx	=	the time and space increments respectively such that $\Delta x/\Delta t >$ free flow speed
$\delta\eta_i$, $\delta\eta_{i+1}$	=	deviations
η	=	state vector
η_i, η_{i+1}	=	state vector at position i, i+1
$f(x, v, t)$	=	vehicular speed distribution function
f	=	relative truck portion, $k_{pass} = k$
f_0	=	equilibrium speed distribution
Γ	=	fluctuating force as a stochastic quantity
g	=	effective green interval
g_j^n	=	is the generation (dissipation) rate at node j at $t = t_0 + n\Delta t$; if no sinks or sources exist g_j^n = 0 and the last term of Equation 5.28 vanishes
$g_{\min}$	=	minimum green time required for undersaturation
h	=	average space headway
i	=	station
j	=	node
k	=	density
k_-, k_+	=	density downstream, upstream shock
k_0	=	operating point
k_{10}	=	equilibrium density
K_A	=	constant value
k_a	=	density within L_2
k_{bumper}	=	density "bumper to bumper"
k_d, q_d	=	density, flow downstream
k_u, q_u	=	density, flow upstream
k_{hom}	=	vehicle density in homogeneous flow
k_j	=	jam density of the approach under consideration
k_j^n, q_j^n	=	density and flow rate on node j at $t = t_0 + n\Delta t$
k_m	=	density conditions
k_{pass}	=	density "bumper to bumper" for 100% passenger cars
k_{ref}	=	reference state
k_{truck}	=	density "bumper to bumper" for 100% trucks
L	=	distance
L	=	length of periodic interval
ld	=	logarithmus dualis
l_o	=	characteristic length
λ	=	wave length of stop-start waves
μ_0	=	dynamic viscosity
μ	=	viscosity term
n	=	current time step
N	=	normalization constant
n_i, n_2	=	exponents
N_i	=	number of cars (volume)
ω	=	eigenvalue
p	=	probability
q	=	actual traffic volume, flow
Q_0	=	net flow rate
q_a	=	average flow rate
$q_a k_a$	=	arrival flow and density conditions
q_{ni}	=	capacity flow
r	=	effective red interval
σ_0	=	quantity
T	=	oscillation time
t	=	time
t_0	=	the initial time
τ	=	relaxation time as interaction time lag
u	=	speed
$U_e(k)$	=	equilibrium speed-density relation
$u_e(k^n_{ij})$	=	equilibrium speed
u_f	=	free-flow speed of the approach under consideration
u_g	=	group velocity
$u_{max} - u_{min}$	=	speed range
u_w	=	shock wave speed
u_z	=	spatial derivative of profile speed
$v(k)$	=	viscosity
v_g	=	values of the group velocity
$W(q)$	=	distribution of the actual traffic volume values q
x	=	space
xh	=	estimated queue length
x_i, t_i, y_i	=	coordinates at point i
X_{ij}	=	length of any line ij
y	=	street width
$y(t)$	=	queue length at any time point t
y_{ij}	=	queue length from i to j assuming a positive direction opposite to x, i.e. from B to A
z	=	$x - U, t$, collective coordinate
$\dot{x}$	=	shockspeed

5.
CONTINUUM FLOW MODELS

5.1 Simple Continuum Models

Looking from an airplane at a freeway, one can visualize the vehicular traffic as a stream or a continuum fluid. It seems therefore quite natural to associate traffic with fluid flow and treat it similarly. Because of this analogy, traffic is often described in terms of flow, concentration, and speed. In the fluid flow analogy, the traffic stream is treated as a one dimensional compressible fluid. This leads to two basic assumptions: a) traffic flow is conserved and; b) there is a one-to-one relationship between speed and density or between flow and density. The first assumption is expressed by the conservation or continuity equation. In more practical traffic engineering terms, the conservation equation implies that in any traffic system input is equal to output plus storage. This principle is generally accepted, and there is no controversy as to its validity.

However, the second assumption has raised many objections in the literature partly because it is not always understood and partly because of contradicting measurements. Specifically, if the speed, u, is a function of density it follows that drivers adjust their speed according to the density, k, (i.e., as density increases with distance then speed decreases). This is intuitively correct, but it can theoretically lead to negative speeds or densities. In addition, it has been observed that for the same value of density many values of speed can be measured. Evidently the assumption has to be qualified. The qualification is that speed (or flow) is a function of density but only at equilibrium. Because equilibrium can rarely be observed in practice, a satisfactory speed-density relationship is hard to obtain, and it is often assumed or inferred theoretically. This particular difficulty has led some researchers to dismiss continuum models or try to oversimplify them. However, as subsequent sections demonstrate, continuum models can be used successfully in simulation and control.

Since the conservation equation describes flow and density as a function of distance and time, one can immediately see that continuum modeling is superior to input-output models used in practice (which are only one dimensional, because they essentially ignore space). In addition, because flow is assumed to be a function of density, continuum models have a second major advantage, (e.g. compressibility). The simple continuum model referred to in this text consists of the conservation equation and the equation of state (speed-density or flow density relationship). If these equations are solved together with the basic traffic flow equation (flow equals density times speed), then we can obtain speed, flow, and density at any time and point of the roadway. Knowing these basic traffic flow variables we know the state of the traffic system and can derive measures of effectiveness, such as delays stops, total travel, total travel time, and others that allow engineers to evaluate how well the system is performing.

As Section 5.1.3 suggests, solution of the simple continuum model leads to the generation of shock waves. *A shock wave is a discontinuity of flow or density, and has the physical implication that cars change speeds abruptly without time to accelerate or decelerate.* This is an unnatural behavior that could be eliminated by considering high order continuum models. These models add a momentum equation that accounts for the acceleration and inertia characteristics of the traffic mass. In this manner, shock waves are smoothed out and the equilibrium assumption is removed (i..e., the high order models apply to non-equilibrium flows since speed is not necessarily the equilibrium speed but is obtained from the momentum equation). In spite of this improvement, the most widely known high order models still require an equilibrium speed-density relationship; recently new high order models were proposed that remove this requirement, but they are largely untested.

It therefore appears that high order models are preferable to the simple continuum; however, their conceptual appeal should be tempered by the difficulty of deriving, calibrating, and implementing a rigorous and practical momentum equation. To be sure, existing literature suggests that the simple continuum model performs better than existing high order models if properly implemented. Intuitively, this could be true when speed flow and density are averaged over long time spans (i.e., in the order of 5 minutes) rather than short ones (i.e., in the order of 30 seconds).

In this chapter, both simple and high order models are presented along with analytical and numerical methods for their implementation. The intent of the chapter is not to reiterate well-known literature reviewed in the previous monograph but rather to summarize the essence of the simple continuum theory for the practicing engineer and demonstrate how it can be implemented in the modeling and analysis of real life situations. With respect to high order models which evolved over the last three decades, we determined that this subject has not been covered adequately; therefore, it is covered in more detail here.

5.1.1 The Conservation Equation

The conservation equation can easily be derived by considering a unidirectional continuous road section with two counting Stations 1 and 2 (upstream and downstream, respectively) as shown in Figure 5.1. The spacing between the two stations is Δx; furthermore, no sinks or sources are assumed within Δx (i.e., there is no generation or dissipation of flow within the section).

Let N_i be the number of cars (volume) passing Station i during time Δt and q_i, the flow passing station i; Δt is the duration of simultaneous counting at Station 1 and 2. Without loss of generality, suppose that $N_1 > N_2$. Because there is no loss of cars in Δx (i.e., no sink), this assumption implies that there is a buildup of cars between Station 1 and Station 2.

Let $(N_2 - N_1) = \Delta N$; for a buildup ΔN will be negative. Based on these definitions we have:
Then the build-up of cars between stations during Δt will be

$$N_1/\Delta_t = q_1 = \textit{flow rate at Station } 1$$
$$N_2/\Delta_t = q_2 = \textit{flow rate at Station } 2$$
$$\Delta N/\Delta t = \Delta_q = \frac{N_2 - N_1}{\Delta t} \Longrightarrow \Delta N = \Delta q \ \Delta t \ .$$

$(-\Delta q)\Delta t$. If Δx is short enough so that density (concentration)k within it is uniform, then the increase in concentration Δk between Stations 1 and 2 during the time interval Δt is

$$\Delta k = \frac{-(N_2 - N_1)}{\Delta x} = \frac{-\Delta N}{\Delta x} \ .$$

This means that the buildup of cars is

$$-\Delta N = \Delta k \Delta x \ .$$

Because cars are conserved

$$-(\Delta q \ \Delta t) = \Delta k \ \Delta x \Longrightarrow \frac{\Delta q}{\Delta x} + \frac{\Delta k}{\Delta t} = 0 \ .$$

If the medium is now considered continuous and the discrete increments are allowed to become infinitesimal, then taking the limit we obtain:

$$\frac{\partial q}{\partial x} + \frac{\partial k}{\partial t} = 0 \qquad (5.1)$$

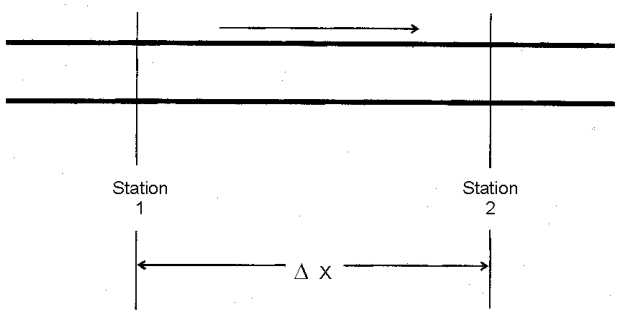

Figure 5.1
Road Section Used for Deriving the Conservation Equation.

$$\frac{\partial q}{\partial x} + \frac{\partial k}{\partial t} = 0 \qquad (5.1)$$

Equation 5.1 expresses the law of conservation of a traffic stream and is known as the conservation or continuity equation. This equation has the same form as in fluid flow. If sinks or sources exist within the section of the roadway, then the conservation equation takes the more general form:

$$\frac{\partial q}{\partial x} + \frac{\partial k}{\partial t} = g(x,t) \qquad (5.2)$$

where $g(x,t)$ is the generation (dissipation) rate in vehicles per unit time per unit length. In practice, generation of cars is observed when flow is interrupted (such as at entrances, exits, or intersections).

Solution of the conservation equation as it applies to traffic flow was first proposed by Lighthill and Whitham (1955) and by Richards (1956). Recently, implementation to traffic analysis simulation and control was proposed by Stephanopoulos and Michalopoulos (1979; 1981).

5.1.2 Analytical Solution of the Conservation Equation; Shock Waves

Equation 5.2 is a state equation that can be used to determine the flow at any section of the roadway. The attractiveness of this equation is that it relates two fundamental dependent variables, density and flow rate, with the two independent ones (i.e., time t, and space x). Solution of Equation 5.2 is impossible without an additional equation or assumption. The first alternative is possible by considering the momentum equation described in Section 5.2. The second option is the one adapted in the simple continuum modeling. It simply states that flow, q, is a function of density, k, i.e., $q = f(k)$. This, or equivalently, $u = f(k)$, is a very reasonable assumption, but it is only valid at equilibrium. For this reason the high order continuum models are, in principle, more appealing but in practice have failed to prove superior to the simple continuum alternative. This is partly because a rigorous form of the momentum equation is hard to derive and partly because its calibration and implementation is still rather complex for most practical applications.

Returning to the solution of Equation 5.2 and considering the fundamental relationship:

$$q = ku \qquad (5.3)$$

we can easily observe that if $u = f(k)$, then in Equation 5.2, we effectively have one equation with only one unknown which can be solved analytically. Analytical solution of the general case is very involved and impractical for real life applications. Therefore, we restrict ourselves only to the pipeline case in which there are no generation or dissipation terms i.e., $g(x,t)=0$. With this in mind, the conservation equation can be rewritten as:

$$\frac{\partial}{\partial x}(ku) + \frac{\partial k}{\partial t} = \frac{\partial}{\partial x}[kf(k)] + \frac{\partial k}{\partial t}$$

$$= f(k)\frac{\partial k}{\partial x} + k\frac{df\partial k}{dk\partial x} + \frac{\partial k}{\partial t} = 0$$

or

$$\left[f(k) + k\frac{df}{dk}\right]\frac{\partial k}{\partial x} + \frac{\partial k}{\partial t} = 0. \qquad (5.4)$$

It should be noted that $f(k)$ can be any function, and that no particular assumptions need to be made in order to keep the results general. For example, if the speed-density relationship is linear as suggested by Greenshields (1934), Equation 5.4 becomes:

$$\left[u_f - 2u_f\frac{k}{k_j}\right]\frac{\partial k}{\partial x} + \frac{\partial k}{\partial t} = 0.$$

where u_f represents the free flow speed and k_j the jam density.

Equation 5.4 is a first order quasi-linear, partial differential equation which can be solved by the method of characteristics. Details of the solution as well as the complete formulation of the

simple continuum modeling were first presented by Lighthill and Whitham (1955). In practical terms, the solution of Equation 5.4 suggests that:

- The density k is constant along a family of curves called characteristics or waves; a wave represents the motion (propagation) of a change in flow and density along the roadway.
- The characteristics are straight lines emanating from the boundaries of the time-space domain.
- The slope of the characteristics is:

$$\frac{dx}{dt} = f(k) + k[f(k)] = \frac{dq}{dk} \tag{5.5}$$

  This implies that the characteristics have slope equal to the tangent of the flow-density curve at the point representing the flow conditions at the boundary from which the characteristic emanates.
- The density at any point x,t of the time space domain is found by drawing the proper characteristic passing through that point.
- The characteristics carry the value of density (and flow) at the boundary from which they emanate.
- When two characteristic lines intersect, then density at this point should have two values which is physically unrealizable; this discrepancy is explained by the generation of shock waves. In short, when two characteristics intersect, a shock wave is generated and the characteristics terminate. A shock then represents a mathematical discontinuity (abrupt change) in k,q, or u.
- The speed of the shock wave is:

$$u_w = \frac{q_d - q_u}{k_d - k_u} \tag{5.6}$$

$$= \frac{time\ \ storage\ \ rate}{space\ \ storage\ \ rate}$$

  where k_d , q_d represent downstream and k_u , q_u upstream flow conditions. In the flow concentration curve, the shock wave speed is represented by the slope of the line connecting the two flow conditions (i.e., upstream and downstream).

It should be noted that when u_w is positive, the shock wave moves downstream with respect to the roadway; conversely, when u_w is negative, the shock is moving upstream. Furthermore, the mere fact that a difference exists in flow conditions upstream and downstream of a point does not imply that a shock wave is present unless the characteristics intersect. Generally this occurs only when the downstream density is higher than upstream. When density downstream is lower than upstream, we have diffusion of flow similar to that observed when a queue is discharging. When downstream density is higher than upstream, then shock waves are generated and queues are generally being built even though they might be moving downstream.

Figure 5.2, taken from Gerlough and Huber (1975), demonstrates the use of traffic waves in identifying the occurrence of a shock wave and following its trajectory. The process follows the steps of the solution of the conservation equation as outlined above. The top of the figure represents a flow-concentration curve; the bottom figure represents trajectories of the traffic waves. On the q-k curve, point A represents a situation where traffic flows at near capacity implying that speed is well below the free-flow speed. Point B represents an uncongested condition where traffic flows at a higher speed because of the lower density. Tangents at points A and B represent the wave velocities of these two situations. The areas where conditions A and B prevail are shown by the characteristics drawn in the bottom of Figure 5.2. This figure assumes that the faster flow of point B occurs later in time than that of point A; therefore, the characteristics (waves) of point B will eventually intersect with those of point A. The intersection of these two sets of waves has a slope equal to the chord connecting the two points on the q-k curve, and this intersection represents the path of the shock wave shown at the bottom of Figure 5.2.

It is necessary to clarify that the waves of the time-space diagram of Figure 5.2 are not the trajectories of vehicles but lines of constant flow and speed showing the propagation of conditions A and B. The velocities of individual vehicles within A and B are higher because the speed of the traffic stream is represented by the line connecting the origin with A and B in the q-k curve.

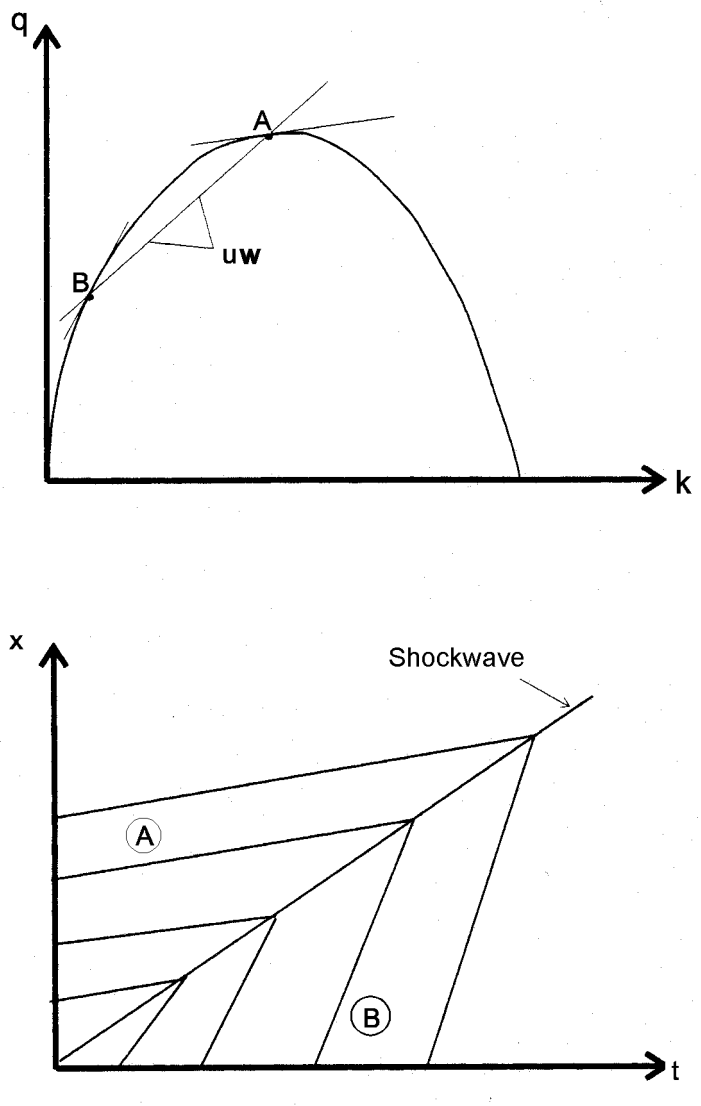

Figure 5.2
Shock Wave Formation Resulting from the Solution of the Conservation Equation.

5.1.3 Applications

Although the simple continuum theory was developed in the mid 50s and is extensively referenced in the literature, it is not widely employed in practice. This is partly because of the lack of understanding of the physical problem under consideration and partly because of difficulties in defining initial and boundary conditions. Furthermore, analytical solutions are not easily obtainable for realistic initial and boundary conditions, complex *u-k* or *q-k* relationships, or interrupted flows. The first problem can be addressed by better understanding the results of the previous section and clearly defining the physical problem. The application of the next section (Stephanopoulos and

Michalopoulos 1979) presents an example of how this can be achieved. It also demonstrates how analytical solutions can be very instructive in better understanding the inner workings of traffic. Other applications of shock waves in signal control, analysis of platoon dynamics, arterial street, and freeway flow can be found in Stephanopoulos and Michalopoulos (1981), Michalopoulos and Pisharody (1980), Michalopoulos (1988), Michalopoulos et al. (1991).

The problem of applying the simple continuum theory in more complex situations, such as interrupted flow, can only be addressed by solving the conservation equation numerically. A numerical approach for implementing the simple continuum modeling is also presented in this chapter. This approach (Michalopoulos et al. 1987) has been employed for analyzing traffic flow in both freeways (Michalopoulos et al. 1991) and arterials (Michalopoulos 1988). The following section only presents an application of the simple continuum modeling to signalized intersections for the purpose of illustrating how the theory can be used to better understand the formation and dissipation of queues. The practical implementation of the theory to freeway and intersection simulation and control can be found in the above-mentioned references.

5.1.4 Formation and Dissipation of Queues at Signalized Intersections

Consider a single-lane queue at the beginning of the effective green at a signalized intersection. If the number of cars in the queue (i.e., the queue size) at this time is x and the average space headway is h, then the estimated queue length (i.e., the space occupied by the x cars) is xh. Suppose now that shortly after the beginning of green, N_1 cars join the queue while N_2 are discharged in front. Then following the same logic, the queue length should be $[x + (N_1 - N_2)]h$. However, generally this is not the case, since shortly after the commencement of green the queue length is growing regardless of the net difference $N_1 - N_2$; for instance, if $N_1 = N_2$ the effective queue size continues to be x, but the queue length can no longer be estimated from the product xh. Clearly, the average space headway is a function of time because of compressibility (i.e., the changing density within the queue in both time and space). This observation leads to the conclusion that although input-output analysis can be used for describing the evolution of queuing situations in time, they yield crude estimations of another important state variable (i.e., the queue length). For fixed-time control such approximations may suffice, but when further accuracy or realism is required, more rigorous modeling is necessary. Another disadvantage of input-output analysis is that the assumption of compact queues leads to miscalculations of the queue size itself and therefore results in miscalculations of delays (Michalopoulos and Pisharody 1981). The simple continuum model offers the advantage of taking compressibility into account since $u = f(k)$ and also it is two dimensional in nature (i.e., in order to obtain the desired results it is necessary to associate traffic flows and densities with time and space).

Application of the simple continuum modeling to this problem begins by definition of boundary and initial conditions which is obtained by examining an approach to a signalized intersection as shown in Figure 5.3, (Stephanopoulos and Michalopoulos 1979). In this figure x,t represent distance and time respectively; it is assumed that within distance L from the stop line there are no entrances or exits. Further it is assumed that L is long enough so that queues do not extend beyond this section and that flow downstream of the stop line is uncongested. Finally, in Figure 5.3, L_1 and L_1' represent the initial and final queue length at the start and end of the cycle c, respectively.

Along the x axis, of Figure 5.3, point B corresponds to the stopline and point A to the tail end of the queue at the beginning of the effective green interval; $t = 0$ corresponds to the start of the effective green. Within AB, jam density and zero flow conditions prevail. Upstream of A and in the remaining portion L_2 of section L, cars arrive at an average flow rate q_a. Thus, density within L_2 is k_a. Assuming an average arrival flow q_a and density k_a during the cycle, then flow and density at the beginning of section L are q_a and k_a during the period $g + r = c$, where c is the cycle length and g,r represent the effective green and red times respectively. Finally, assuming that the cycle is saturated, capacity flow and density conditions q_m and k_m prevail at the stopline during g (i.e., from point B to point F) while during the effective red flow, at the stopline (point F to end of cycle) is congested (i.e., $q = 0$ and $k = k_j$). The characteristic lines emanating from $t = 0$, $x = 0$, and $x = L$ were drawn based on this definition of initial and boundary conditions. These lines are tangent to the flow-versus-density curve evaluated at the flow and density conditions corresponding to the point of origin.

For example, within AB, the slope of the characteristics is negative, and it is the same as the tangent at the point $0,k_j$ of the flow-density curve, where k_j represents the jam density. To

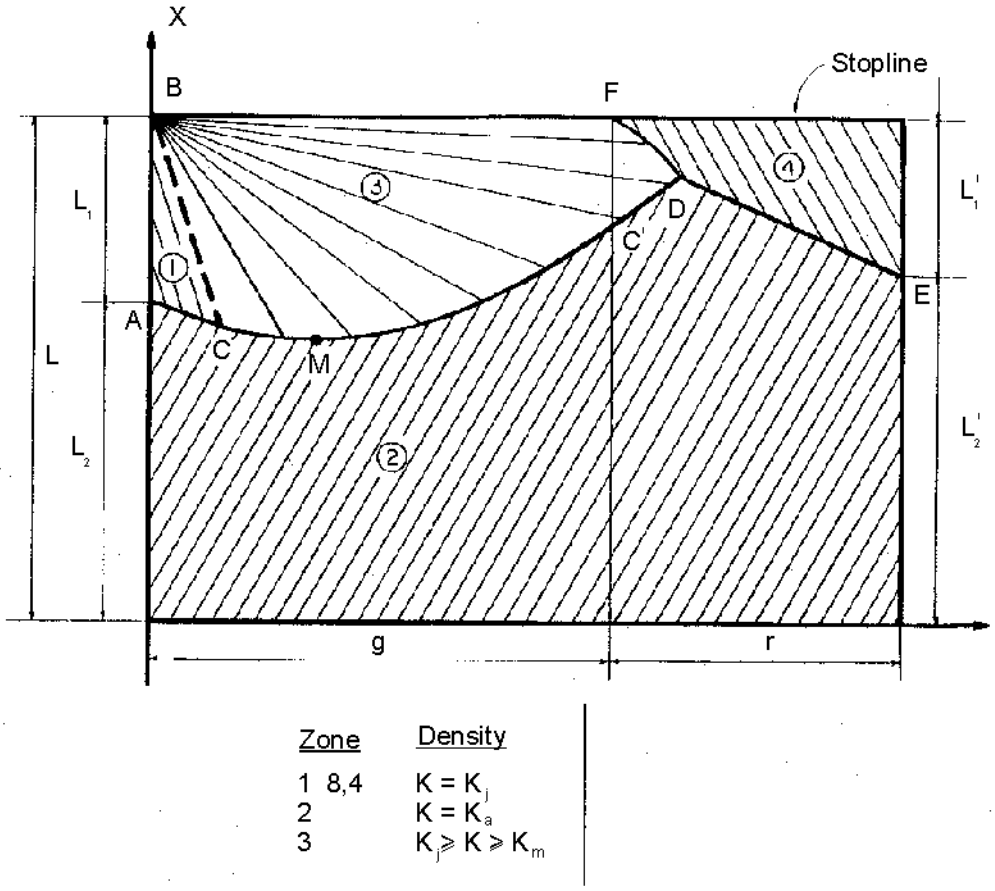

Figure 5.3
Queue Length Developments at a Signalized Intersection During a Saturated Cycle.

visualize this, one can imagine the simple flow density curve resulting from the Greenshields (1934) model shown at the right of Figure 5.4. At point B, density changes instantaneously from k_j to k_m , where k_m is density at capacity; therefore, the characteristics at B fan out (i.e., they take all possible slopes from $(dq/dk)_{0',kj}$ to zero). Proceeding in this fashion, one can draw the remaining characteristics as shown in Figure 5.3.

The characteristic lines emanating from the boundaries divide the entire time-space domain $[0 \leq x \leq L,\ 0 \leq t \leq c]$ into four distinct zones of different flow and density conditions as shown in Figure 5.3. When the characteristics intersect, ashock wave is generated. At the tail end of the queue, shock wave ACMDE is generated during the period of one cycle; therefore, this line represents the trajectory of the tail end of the queue and its vertical distance to the stopline represents queue length denoted as $y(t)$. The slope of line ACMDE at any point represents the speed at which this shock wave (or, equivalently, the tail end of the queue) propagates upstream or downstream of the roadway.

Derivation of the queue tail trajectory proceeds by examining the intersection of the characteristics. To begin with, it can be seen that at point A, a linear shock wave is generated moving backwards with respect to the stop line. This shock ends at C since line BC represents the last characteristic carrying density k_j emanating from the stop line. After C, density downstream of the shock is variable due to the varying densities carried by the fanning characteristics of zone 3 while density upstream of the shock is constant k_a. This is the reason the shockwave CMD is nonlinear, in fact, it moves with variable speed as shown by the slope of line CMD. At the end of the effective green (point F),

shock wave FD is generated and meets the tail end of the queue at point D. Again, this shock moves with variable speed as density
downstream of it (Zone 4) is constant and equals to k_j while upstream (Zone 3) density varies between k_j and k_m. At point D, a linear slack similar to AC takes over. Finally, at the end of the cycle, the distance L_1' represents the final queue length, or, equivalently, the initial queue length of the next cycle.

It should be noted that if the cycle is undersaturated, line ACMD intersects the stopline during green and point D falls on the stopline; after point D, the queue length is zero. In this case, for the remainder of the green interval, vehicles depart without delay; at point F, the queue length starts increasing again linearly until the end of the cycle. This as well as other complexities, such as gradual transition to capacity or the presence of sinks and sources are discussed in Stephanopoulos and Michalopoulos (1979) and Michalopoulos (1988).

5.1.4.1 Analytical Results

Each segment of line ACMDE and the coordinates of points C, M, D and E can be derived analytically. In order to obtain analytical results, one must assume a specific relationship between flow and density or, equivalently, between speed and density. For simplicity, the linear speed-density model (Greenshields 1934) can be assumed, but it should be noted that similar results can be obtained for any other model. The trajectory of the queue length in Figure 5.3 was derived by using the following notation (Stephanopoulos and Michalopoulos 1979):

- $y(t)$ = queue length at any time point t,
- g = effective green interval,
- r = effective red interval,
- c = $g + r$ = cycle length,
- g_{min} = minimum green time required for undersaturation,
- X_{ij} = length of any line ij,
- u_f = free-flow speed of the approach under consideration,
- k_j = jam density of the approach under consideration,
- q_a, k_a = arrival flow and density conditions,
- x_i, t_i, y_i = coordinates of point i, and consideration,
- y_{ij} = queue length from i to j assuming a positive direction opposite to x, i.e. from B to A (Figure 5.3).

Based on the earlier discussion the following analytical expressions can be obtained for the queue length and dissipation times (Stephanopoulos and Michalopoulos 1979):

$$X_{BC} = L - u_f t \tag{5.7}$$

$$X_{AC} = (L - L_1) - [(k_a u_f / k_j)]t \tag{5.8}$$

$$X_C = L - [k_j L_1 / (k_j - k_a)] \tag{5.9}$$

$$t_C = [k_j L_1 / u_f (k_j - k_a)] \tag{5.10}$$

$$y_C = [k_j L_1 / (k_j - k_a)] = L - X_c \tag{5.11}$$

$$y_{CMD} = [u_f + h(k_a)](tt_c)^{1/2} - h(k_a)t \tag{5.12}$$

$$h(k_a) = u_f[1 - (2k_a/k_j)]$$

$$t_M = [u_f + h(k_a)]^2 t_C / 4[h(k_a)]^2 \tag{5.13}$$

$$y_M = [u_f + h(k_a)]^2 t_C / 4[h(k_a)] \tag{5.14}$$

$$y_{FD} = u_f t - u_f (tg)^{1/2} \tag{5.15}$$

$$t_D = \{(t_C)^{1/2} + [u_f (g)^{1/2} / u_f + h(k_a)]\}^2 \tag{5.16}$$

$$y_D = u_f \{t_C - [u_f h(k_a) g] / [u_f + h(k_a)]^2 + [u_f - h(k_a)](gt_C)^{1/2} / [u_f + (k_a)] \} \tag{5.17}$$

$$y_{DE} = y_D + [u_f k_a (t - t_D) / k_j] \tag{5.18}$$

$$y_E = L_1' = L_1 + [(k_a u_f c)/k_j] - [k_j u_f g]/4(k_j - k_a) \tag{5.19}$$

$$t_E = c \tag{5.20}$$

In an undersaturated cycle, the queue dissipates in time:

$$g_{\min} = [(y_C / t_C) + h(k_a)]^2 t_C / [h(k_a)]^2 \tag{5.21}$$

This is the minimum green time required to dissolve the initial queue L_1. In such a cycle, the final queue length L_1' is independent of the initial L_1 and is given by:

$$y_E = L_1' = (c - g)(k_a u_f)/k_j \tag{5.22}$$

Details such as gradual transition to capacity at point B and capacity drops during green can also be taken into account.

5.1.4.2 Queue Length Stability

The analytical relations between the initial and final queue developed in the preceding section can be used for stability analysis in saturated cycles. Equation 5.19 can be rewritten as

$$L_1' = L_1 + b \tag{5.23}$$

where

$$b = (k_a u_f c/k_j) - [k_j u_f g/4(k_j - k_a)] \tag{5.24}$$

If c and g are given, b is constant, i.e., it is independent of the initial queue L_1. Thus, Equation 5.23 can be generalized for any cycle N and rewritten as

$$L_{N+1} = L_N + b \tag{5.25}$$

where L_N and L_{N+1} are the queues at the beginning of cycle N and N+1. Clearly, a steady state exists if $L_N = L_{N+1}$ or if $L_N = L_N + b$, i.e., if $b = 0$. Therefore, for steady state:

$$(k_a u_f c/k_j) - [k_j u_f g/4(k_j - k_a)] = 0 \tag{5.26}$$

and solving for g/c:

$$g/c = [k_j g/4(k_j - k_a)] = \lambda \tag{5.27}$$

Since λ is positive, it is easily seen that if $g/c < \lambda$, the queue length at the end of the cycle will be growing for as long as this situation persists. Otherwise, if $b < 0$ or, equivalently, if $g/c > \lambda$, the queue at the end of the cycle will decrease. It should be noted that Equations 5.25 and 5.27 are meaningful for saturated cycles (i.e., for green times less than the ones given by Equation 5.21). Otherwise, L_{N+1} is not related to L_N and it is given from Equation 5.22. A final note concerning the stability of the steady state is worthy of emphasis. As Equation 5.25 reveals, the steady state is metastable. If $b = 0$, a small variation of the demand will change the steady state to a nearby value that is also metastable. Therefore, the queue length at the beginning of each cycle will change according to the fluctuating values of b, which depend on the demand.

5.1.4.3 Signalized Links and Platoon Behavior

Extension to similar analytical results for a system of intersections is a rather complex analytical exercise, but it is very useful in obtaining an insight of the nature of the problem. Figure 5.4 presents just a possibility of queue length and shock wave developments at a signalized link during a saturated cycle. Line $A_3,C_3,M_3,D_3,E_3,F_3,H_3$ corresponds to the downstream queue, and its trajectory can be determined analytically (Michalopoulos et al. 1980). Since the number of possibilities is very large even under simplifying assumptions, one can see that we have to turn to numerical methods for solving the conservation equation at complex situations.

A major benefit of the continuum modeling is the fact that compressibility is built into the state equations since speed or flow is assumed to be a function of density. This suggests that as groups of cars enter areas of higher density, the continuum models exhibit platoon compression characteristics; conversely, when they enter areas of lower density we observe diffusion or dispersion. This phenomenon has been shown analytically in Michalopoulos and Pisharody (1980), where it is demonstrated that by using continuum models we do not have to rely on empirical dispersion models such as the ones employed today in most signal control packages. The result is a more realistic and elegant modeling that should lead to more effective control.

5.1.5 Numerical Solution of the Conservation Equation

The advantage of the analytical results presented thus far is that they visually depict the effects of downstream disturbances on upstream flow. Thus they provide a good insight on the formation and dissipation of queues and congestion in time and space in both freeways and arterials; further, they can be used to demonstrate that platoon dispersion and compression are inherent in this modeling (i.e., it does not have to be induced externally). The disadvantage of the analytical solution lies in the oversimplifications needed in the derivations.

These include simple initial flow conditions, as well as arrival and departure patterns, absence of sinks or sources, and uncomplicated flow-concentration relationships. Most importantly, complexities frequently encountered in real

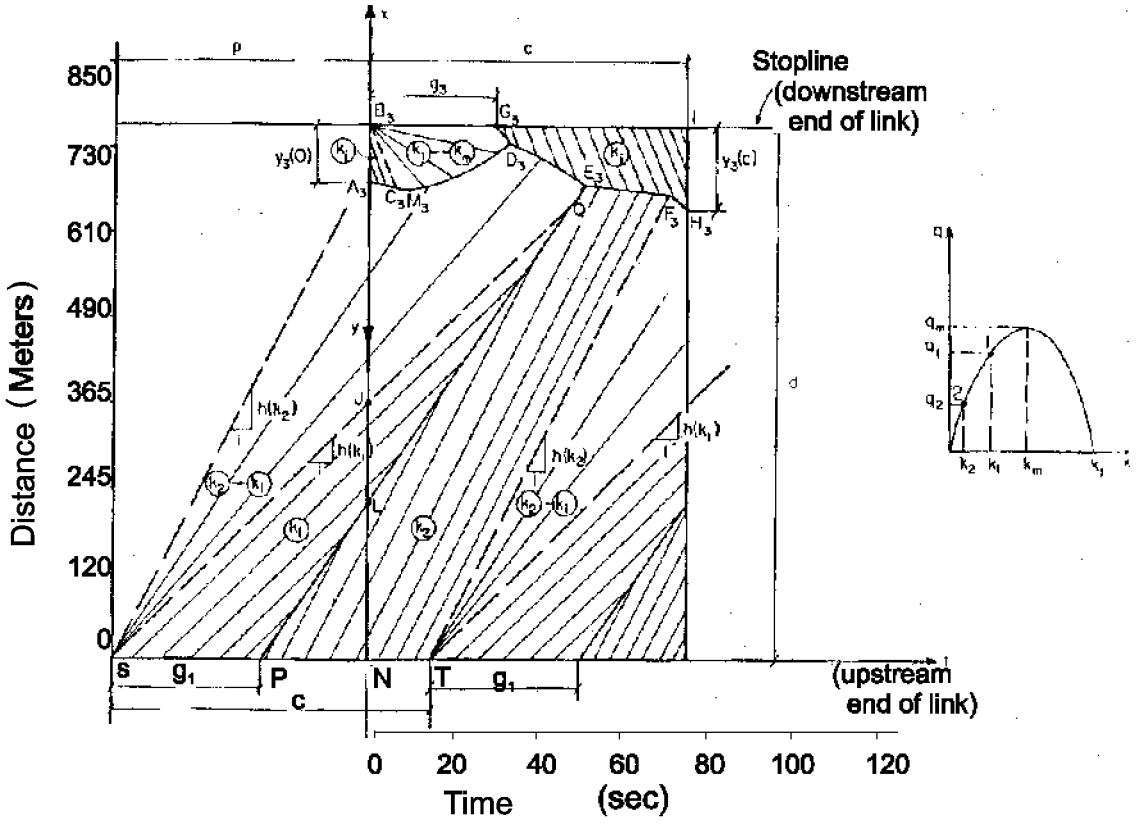

Figure 5.4
Shock Wave Developments Between Two Signalized Intersections During a Saturated Downstream Cycle.

situations such as turning lanes, side streets, or freeway entrances and exits cannot be treated analytically with ease. As in similar problems of compressible flow, these difficulties can be resolved by developing numerical solutions for the state equations. Clearly, a numerical methodology is needed for numerical implementation of the conservation equation in practical situations. This allows for inclusion of complexities one is likely to encounter in practice (turning lanes, sinks and sources, spillbacks, etc.) treatment of realistic arrival and departure patterns, more complicated *u-k* models, as well as inclusion of empirical considerations. Numerical computation of *k, u*, and *q* proceeds by discretizing the roadway under consideration into small increments Δx (in the order of 9 to 45 meters) and updating the values of these traffic flow variables on each node of the discretized network at consecutive time increments Δt (in the order of one second or so).

Space discretization of a simple signalized traffic link without side streets is presented in Figure 5.5 in which the dashed segments represent dummy links that are necessary in the modeling in this application (Michalopoulos 1988). It should be emphasized that this discretization is not physical and is only performed for computational purposes. Referring to the solid segments, density on any node *j* except the boundary ones (i.e., 1 and *J*) at the next time step *n+1* is computed from density in the immediately adjacent cells (both upstream and downstream *j*-1 and *j*+1 respectively) at the current time step *n* according to the relationship:

$$k_j^{n+1} = \frac{1}{2}(k_{j+1}^n + k_{j-1}^n) - \frac{\Delta t}{2\Delta x}(q_{j+1}^n - q_{j-1}^n) + \frac{\Delta t}{2}(g_{j+1}^n + g_{j-1}^n) \quad (5.28)$$

in which:

k_j^n, q_j^n	=	density and flow rate on node j at $t=t_0+n\Delta t$
t_0	=	the initial time
Δt, Δx	=	the time and space increments respectively such that $\Delta x/\Delta t >$ free flow speed.
g_j^n	=	is the generation (dissipation) rate at node j at $t = t_0+n\Delta t$; if no sinks or sources exist $g_j^n = 0$ and the last term of Equation 5.28 vanishes.

Once the density is determined, the speed at $t+\Delta t$ (i.e., at $n+1$) is obtained from the equilibrium speed density relationship $u_e(k)$, i.e.,

$$u_j^{n+1} = u_e(k_j^{n+1}) \quad (5.29)$$

For instance, for the Greenshields (1934) linear model,

$$u_j^{n+1} = u_f\left(1 - \frac{k_j^{n+1}}{k_{jam}}\right) \quad (5.30)$$

where u_f is the free flow speed and k_{jam} the jam density. It should be noted that Equation 5.28 is applicable for any speed density model including discontinuous ones; if an analytical expression is not available, then u can easily be obtained numerically from the u-k curve. Finally, flow at $t+\Delta t$ is obtained from the fundamental relationship:

$$q_j^{n+1} = k_j^{n+1} u_j^{n+1} \quad (5.31)$$

in which, the values of k and u are first obtained from Equations 5.28 and 5.29. It can be demonstrated (Michalopoulos 1988) that measures of effectiveness such as delays, stops, total travel, etc., can be derived from k, u, and q. Further, the generation term can either be measured (e.g., by detection devices) or more practically estimated in each time step (Michalopoulos 1988; Michalopoulos et al. 1991). It is important to note that Equation 5.28 allows congestion to propagate both upstream and downstream rather than upstream only.

It should be evident that the above solution requires definition of the initial state of the system (i.e., the values of k, u, and q at $t=t_0$) as well as boundary conditions, (i.e., k and q at $j=1$ and $j=J$, upstream end of the link and stopline respectively). However, this is essential for analyzing flow regardless of the modeling and solution method (i.e., arrivals and departures at the boundaries and initial flows must always be specified). For practical implementation of Equations 5.28, 5.29, and 5.31, one only needs to specify arrival and departure flow rates; density at $j=1$ and $j=J$ is obtained from an equilibrium q-k model. The discretization of Figure 5.5 and numerical solution of this section assume that all space increments Δx are equal. Variable space discretization is also possible; however, regardless of the discretization scheme the relationship $\Delta x/\Delta t > u_f$ must be maintained at all times for convergence. Finally, direct measurement of density and initial and boundary conditions can be obtained by wide area detection devices that were only recently developed and implemented in the field (Michalopoulos et al. 1992). This is particularly important for measuring and periodically updating initial conditions.

In conclusion it is noted that more accurate numerical methods can be developed for solving the conservation Equation 9; such methods are not recommended as they lead to sharp shocks which are unrealizable in practice. This along with numerical examples and applications are discussed in the references cited earlier. One of the most interesting applications is the one in which the simple continuum model is implemented for analyzing multiple lane flows (Michalopoulos et al. 1984). The modeling is relatively simple, but it can only be implemented by numerical methods.

5.1.6 Application to Multi-Lane Flow Dynamics

A simple continuum model for describing flow along two or more homodirectional lanes can be obtained by considering the

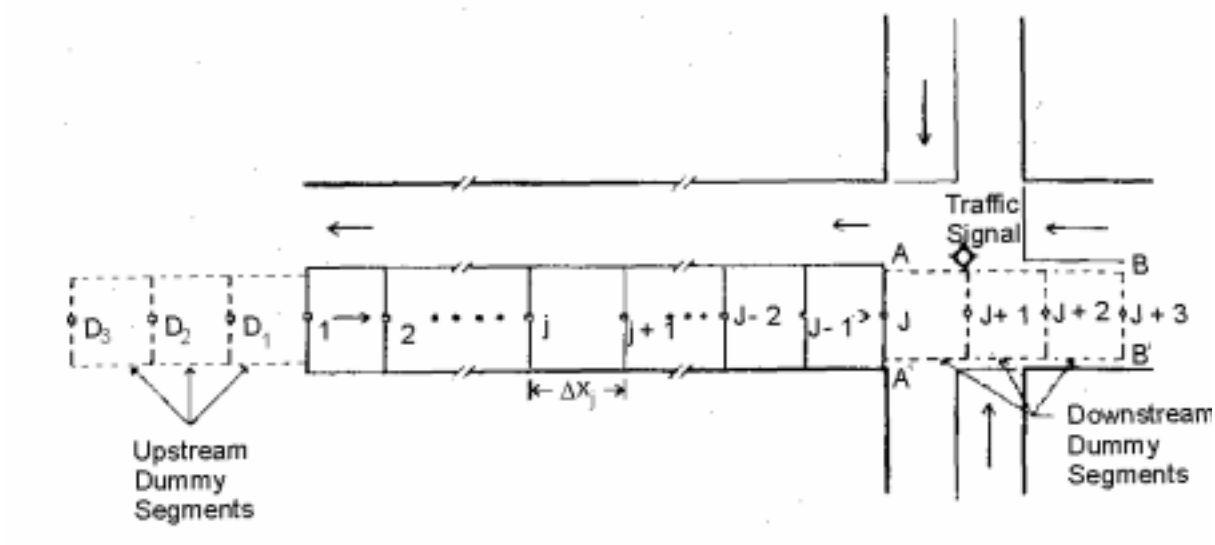

Figure 5.5
Space Discretization of a Simple Link.

conservation equation of each lane. This is accomplished by observing that the exchange of flow between lanes represents generation (or loss) of cars in the lane under consideration. The generation term is obtained from the assumption that the exchange of vehicles between two neighboring lanes is proportional to the difference of the deviations of their densities from equilibrium values (Gazis et al. 1962). These values are known lane-specific constants which can be obtained experimentally. Based on these considerations, the following system describes flow on a two lane freeway (Munjal and Pipes 1971).

$$\frac{\partial q_1}{\partial x} + \frac{\partial k_1}{\partial t} = Q_1$$

$$\frac{\partial q_2}{\partial x} + \frac{\partial k_2}{\partial t} = Q_2$$

where, t and x are the time and space coordinates, respectively; $q_i(x,t)$ is the flow rate of the ith lane (i = 1, 2); k (x,t) is the density of the ith lane (i = 1, 2); and $Q_i(x,t)$ is the lane changing rate (i = 1, 2). From the assumptions stated above

$$Q_1 = \alpha[(k_2 - k_1) - (k_{20} - k_{10})]$$
$$Q_2 = \alpha[(k_1 - k_2) - (k_{10} - k_{20})]$$

where α is a sensitivity coefficient describing the intensity of interaction, having units of time^{-1}; k_{10} is the equilibrium density of the ith lane. Since the system is conserved it can be easily seen that $Q_1 + Q_2 = 0$.

The above formulation does not take into account generation or loss of cars that are introduced at entrance or exit ramps. In addition, when densities are equal lane changing will occur if $k_{10} \neq k_{20}$. While this formulation results in lane changing even at very low densities, this is a rather rare behavior at nearly free flow conditions (assuming no generation of cars). A simple improvement would be to assume that the sensitivity coefficient, α, depends on the difference in density between the two lanes rather than being constant. With this improvement and the inclusion of sinks and sources as well as an interaction time lag (Gazis et al. 1962), the previous formulation can be modified to:

$$\frac{\partial q_1}{\partial x} + \frac{\partial k_1}{\partial t} = g + Q_1 \qquad (5.32)$$

$$\frac{\partial q_2}{\partial x} + \frac{\partial k_2}{\partial t} = Q_2 \qquad (5.33)$$

where $g(x,t)$ is the generation rate in lane 1; at exit ramps g is negative.

$$Q_1 = \alpha[\{k_2(x, t-\tau) - k_1(x, t-\tau)\} - (k_{20} - k_{10})];$$
$$Q_2 = \alpha[\{k_1(x, t-\tau) - k_2(x, t-\tau)\} - (k_{10} - k_{20})],$$

where

$$\alpha = \begin{cases} 0, & |k_2(x,t-\tau) - k_1(x,t-\tau)| \le k_A \\ \left(\frac{\alpha_{max}}{k_0 - k_A}\right) |(k_2(x,t-\tau) - k_1(x,t-\tau)| - K_A), & |k_2(x,t-\tau) - k_1(x,t-\tau)| > k_A \end{cases} \quad (5.34)$$

k_A is a constant value below which no exchange of flow occurs; τ is the interaction time lag, and k_0 the jam density.

In this formulation it is assumed that cars are generated in (or depart from) lane 1 (i.e. the right lane of the highway). A similar generation term could also be added to lane 2 if appropriate. The system of governing equations (Equations 5.32 and 5.33) can be solved numerically by discretizing in time and space (Michalopoulos et al. 1984). Figure 5.6 presents space discretization of a two lane freeway section including an entrance ramp; multiple entrances and exits can be treated similarly. Following guidelines similar to those of Section 5.1.5, a numerical solution of Equations 5.32 and 5.33 is (Michalopoulos et al. 1984):

$$k_{1,j}^{n+1} = \frac{1}{2}(k_{1,j+1}^{n} + k_{1,j-1}^{n}) - \frac{\Delta t}{2\Delta x}(G_{1j-1}^{n} - G_{1j-1}^{n}) + \frac{\Delta t}{2}(g_{1,j+1}^{n} + g_{1,j-1}^{n}) + \frac{\Delta t}{2}(Q_{1,j+1}^{n} + Q_{1,j-1}^{n}),\ j = 1,2,...,J \quad (5.35)$$

$$k_{2,j}^{n+1} = \frac{1}{2}(k_{2,j+1}^{n} + k_{2,j-1}^{n}) - \frac{\Delta t}{2\Delta x}(G_{2,j+1}^{n} - (Q_{2,j+1}^{n} + Q_{2,j-1}^{n}),\ j = 1,2,. \quad (5.36)$$

where $k_{i,j}^{n}$: the density of the ith lane and the jth node at $t = t_0 + n \cdot \Delta t$; t_0 = the initial time

$$Q_{1,j}^{n} = \alpha_{1,j}^{n-s}[(k_{2,j}^{n-s} - k_{1,j}^{n-s}) - (k_{20} - k_{10})]$$

$$Q_{2,j}^{n} = \alpha_{2,j}^{n-s}[(k_{1,j}^{n-s} - k_{2,j}^{n-s}) - (k_{10} - k_{20})]$$

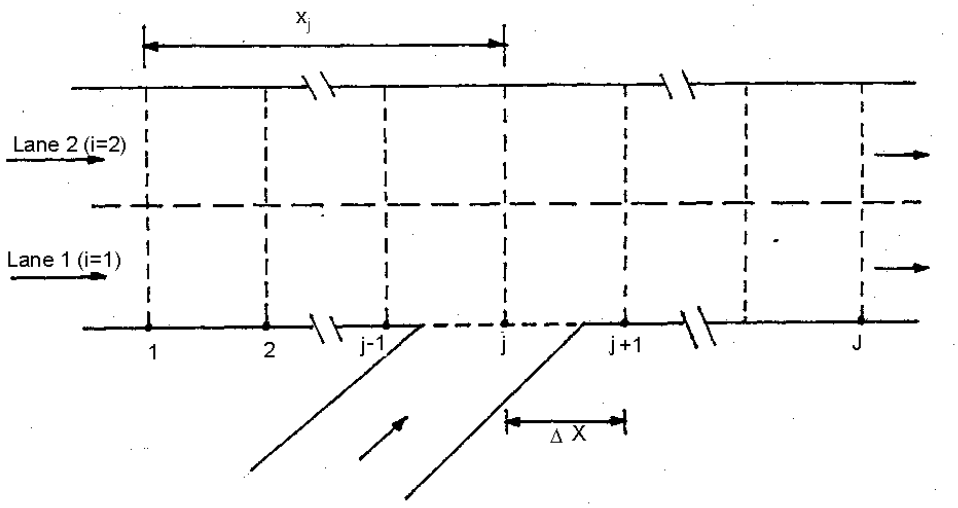

Figure 5.6
Space Discretization of a 2-Lane, One Dimensional Freeway Section.

,

$$G_{i,j}^{n} = k_{i,j}^{n} \cdot u_{i,j}^{n} = k_{i,j}^{n} \cdot u_e(k_{i,j}^{n}) \qquad (i = 1,2)$$

$u_e(k^n_{i,j})$ is the equilibrium speed corresponding to $k_{i,j}^{n}$; assuming the simple equilibrium model of Greenshields (1934) it can be easily verified that $G^n_{i,j} = k^n_{i,j} u_f (1 - (k^n_{i,j}/k_0))$ where u_f and k_0 represent the free flow speed and jam density, respectively.

Following computation of density at each time step, the flow rate $q_{i,j}^{n+1}$ and speed $u^n_{i,j}$ are obtained from

$$u_{i,j}^{n+1} = u_e(k_{i,j}^{n+1})$$

and

$$q_{i,j}^{n+1} = k_{i,j}^{n+1} u_{i,j}^{n+1} \ .$$

The upstream or downstream boundary conditions ($k^n_{1,j}$; $k^n_{i,j}$) required in the solution correspond to the arrivals or departures, and they can be constant, time varying, and/or stochastic; the latter can be generated numerically by simulation techniques. Initial conditions can be either constant or varying with space depending on the particular situation under consideration. Further, at the downstream boundary when flow is unspecified and Δx is sufficiently small, it can be assumed that;

$$k_{i,J}^{n} = k_{i,J-1}^{n-1} \qquad \forall_n;\ i = 1,2$$

Finally, during the initialization period $0 \le t \le \Delta\tau$,(i.e., when $n - s \le 0$) it can be assumed that $\alpha_{i,j}^{n-s} = 0$, implying no exchange of flow between lanes.

Extension of the simple continuum modeling to more than two lanes is straightforward. If I represents the number of lanes, the general conservation equation of each lane is

$$\frac{\partial q_i}{\partial x} + \frac{\partial k_i}{\partial t} = g_i + Q_i \qquad i = 2,3,...,I \ . \tag{5.37}$$

where

$$\begin{aligned} Q_i = {} & \alpha_{i,i-1}[\{k_{i-1}(x,t-\tau) - k_i(x,t-\tau)\} - (k_{(i-1)0} - k_{i0})] \\ & + \alpha_{i,i+1}[\{k_{i+1}(x,t-\tau) - k_i(x,t-\tau)\} - (k_{i+1,0} - k_{i0})] \end{aligned} \tag{5.38}$$

$g_i = 0$ for all internal lanes, i.e. for $i = 2,3,..., I - 1$

$$\alpha_{i,j\pm1} = \begin{cases} 0 & |k_i(x,t-\tau) - k_{i\pm1}(x,t-\tau)| \le k_A \\ \dfrac{\alpha_{\max}}{k_0 - k_A}|k_i(x,t-\tau) - k_{i\pm1}(x,t-\tau)| - k_A), & \\ |k_i(x,t-\tau) - k_{i\pm1}(x,t-\tau)| > k_A \end{cases}$$

alternatively

$$\alpha_{i,i\pm1} = constant$$

The above equations are also valid for the first and last lanes ($i = 1$ and $i = I$); in these cases one should set $i - 1 = i$ for $i = 1$; $i + 1 = i$ for $i = I$ and $g_i = f(x,t)$.

Following a similar notation as before, the general solution of Equation 5.37 is:

$$\begin{aligned} k_{i,j}^{n+1} = {} & \frac{1}{2}(k_{i,j+1}^{n} + k_{i,j-1}^{n}) - \frac{\Delta t}{2\Delta x}(G_{i,j+1}^{n} - G_{i,j-1}^{n}) + \frac{\Delta t}{2}(g_{i,j}^{n} \\ & + \frac{\Delta t}{2}(Q_{i,j+1}^{n} + Q_{i,j-1}^{n}) \quad i = 1,2,.....,I \end{aligned}$$

where

$$\begin{aligned} Q_{i,j}^{n} = {} & \alpha_{i,j}(k_{i,j}^{n-s}, k_{i-1j}^{n-s})[(k_{i-1j}^{n-s} - k_{i,j}^{n-s}) - (k_{(i-1)0} - k_{i,0})] \\ & + \alpha(k_{i,j}^{n-s}, k_{i+1,j}^{n-s})[(k_{i+1,j}^{n-s} - k_{i,j}^{n-s}) - (k_{(i+1)0} - k_{i0})] \end{aligned}$$

$$G_{ij}^{n} = k_{i,j}^{n} \cdot u_{i,j}^{n} = k_{i,j}^{n} u_e(k_{i,j}^{n})$$

$$\alpha(k_i^{n-s}, k_{i\pm1}^{n-s}) = \begin{cases} 0 & |k_{i,j}^{n-s} - k_{i\pm1,j}^{n-s}| \le k_A \\ \dfrac{\alpha_{\max}}{k_0 - k_A}(|k_{i,j}^{n-s} - k_{i\pm1,j}^{n-s}| - k_A) & |k_{i,j}^{n-s} - k_{i\pm1,j}^{n-s}| > k_A \end{cases}$$

The models presented to this point did not include the street width y, explicitly (i.e., they were discrete with respect to this spatial dimension). This discretization appears natural due to the division of the road surface in lanes. However, during the lane changing process, flow and speed exhibit a second component parallel to the y dimension. In principle, a two dimensional formulation with respect to space should more adequately describe the traffic flow process. A simple continuum formulation based on the law of conservation alone is

$$\frac{\partial k}{\partial t} + \frac{\partial (k u_x)}{\partial x} + \frac{\partial (k u_y)}{\partial y} = g(x,y,t) \qquad (5.39)$$

x, y, t are the space and time coordinates, respectively; $k = k(x,y,t)$ = the traffic density; $u_x = u_x(x,y,t)$ = the x component (parallel to the road axis) of the velocity vector; $u_y = u_y(x,y,t)$ = the y component of the velocity vector; $g(x,y,t)$ is the generation rate.

Since the above equation has three unknowns, it must be combined with two equations of state of the form

$$u_x = u_x(x,y,t) = u_e(k)$$

$$u_y = u_y(x,y,t) = v_e(k).$$

It should be noted that in this new formulation, density represents the number of cars per unit area; for instance jam density is defined as:

$$\overline{k}_0 = \frac{1}{h_x h_y}$$

where h_x, h_y are the minimum space headways in each direction x and y respectively.

The general conservation form of Equation 5.39 is

$$k_t + (k u_x)_x + (k u_y)_y = g \qquad (5.40)$$

Again Equations 5.39 and 5.40 can be solved numerically, and expressions for $u_e(k)$ and $v_e(k)$ can be obtained (Michalopoulos 1984).

5.2 High Order Models

5.2.1 Criticism of Simple Continuum Models

The simple continuum models used in the previous section resulted in the kinematic wave description of traffic flow. However, these models have some shortcomings which are given in the following list:

- Kinematic models contain stationary speed-density relation (i.e., the mean speed should adjust instantaneously to traffic density) more realistic is that speed is adapted after a certain time delay and to reflect traffic conditions downstream.

- Kinematic wave theory shows shock wave formation by steeping speed jumps finally to infinite sharp jumps. A macroscopic theory is based on values which are average values from an ensemble of vehicles. Averages are taken either over temporal or spatial extended areas. Infinite jumps, therefore, are in contradiction to the basics of macroscopic description. The only solution is to include noninstantaneous adjusting of speed-flow characteristics by an additional acceleration equation, which at the end introduces diffusion and smears out sharp shocks (compare Figure 5.7).

- Unstable traffic flow is characterized under appropriate conditions by regular stop-start waves with amplitude-dependent oscillation time. Oscillatory solutions cannot be derived from kinematic wave equations.

- The dynamics of traffic flow result in the hysteresis phenomena. This consists of a generally retarded behavior of vehicle platoons after emerging from a disturbance compared to the behavior of the same vehicles approaching the disturbance (compare Figure 5.7). Simple continuum models cannot describe such

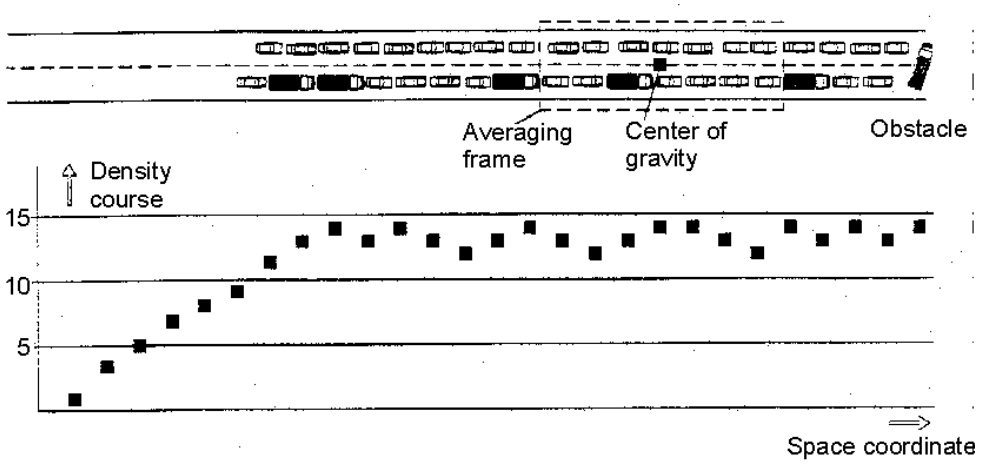

Note: Macroscopic Models are based on temporal and spatial average values which do not lead to sharp shocks even in the case of vehicles distributed like a heaviside step function.

Figure 5.7
Macroscopic Models.

phenomena. In Figure 5.8, hysteresis phenomenon is an example of dynamic behavior of traffic flow which cannot be covered by simple kinematic traffic wave theory. Volume and density represented by the observed platoon are different after emerging from a kinematic disturbance compared with the platoon approaching the disturbance. Data from aerial survey recording (Treiterer and Myers 1974; Treiterer 1973).

- Besides hysteresis, the crucial instability effect is bifurcation behavior (i.e., traffic flow becomes unstable beyond a certain critical traffic density). Once overcrossing the critical density, the traffic flow becomes rapidly more congested without any obvious reason. Kinematic traffic wave theory can only show that wave propagation direction can change from downstream to upstream.

- Finally, with the dynamics of traffic flow the deviations of measured state points from the approximating curve for the speed-density relation can be explained not only as stochastic effects. To dispense a dynamic description by using a steady state speed-density characteristic mixes stationary and non-stationary measured traffic state points. Since the speed-density relation as an operating line is essential for the design of all sorts of traffic control, this mixing is highly questionable.

The significant shortcomings of the simple continuum models suggest the justification for a dynamic extension leading to an improved description of traffic flow.

5.2.2 Transients and Stop-Start Waves

Before developing detailed higher order continuum model (taking into account acceleration and inertia effects by regarding non-instantaneous and spatially retarded reactions), experimental observations are reported such as transients and the formation of stop-start waves.

The most impressive measurements of transients and stop-start wave formation are gained from European freeways. Due to space restrictions, there are numerous freeways with two lanes per highwayin Europe. These freeways, often equipped with a dense measurement grid not only for volume and occupancy but also for speed detection, show stable stop-start waves lasting in some cases for more than three hours. Measurement data exists for Germany (Leutzbach 1991), the Netherlands (Verweij 1985), and Italy (Ferrari 1989). At first, the German data are reported.

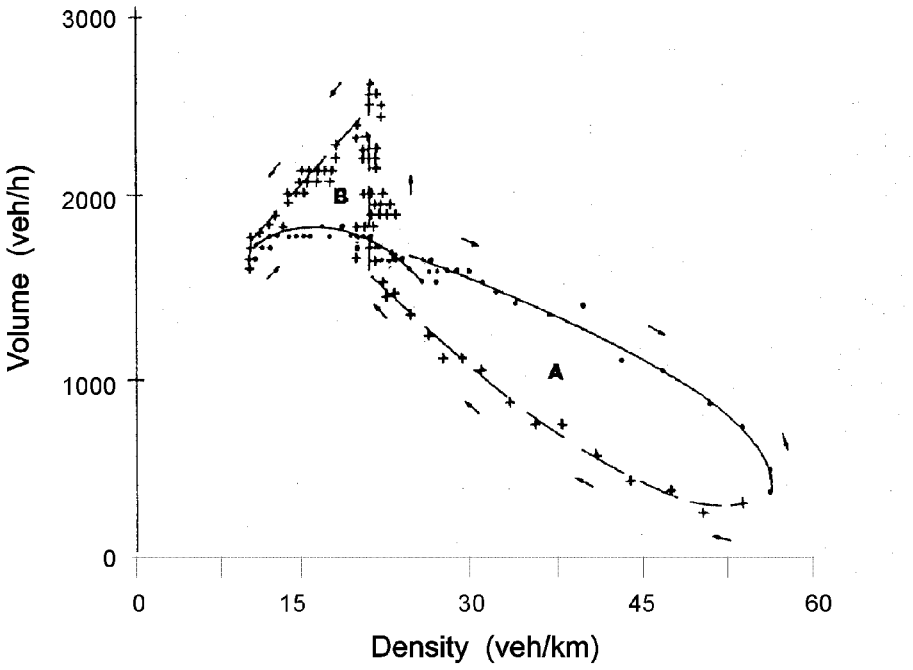

Figure 5.8
Hysteresis

Phenomenon as an Example
of Dynamic Behavior of Traffic Flow.

The series are recorded from the Autobahn A5 Karlsruhe-Basel at 617 km by the Institute of Transport Studies at Karlsruhe University (Kühne 1987). Each measurement point is a mean value of a two-minute ensemble actuated every 30 sec. The dates stem from holiday traffic with no trucks.

All reported cases have densities beyond the critical density and show unstable traffic flow (i.e., stop-start waves with more or less regular shape and of long duration - in some series up to 12 traffic breakdowns). It is possible to draw in each measurement series and idealized strongly periodic stop-start waves and to collect the resulting amplitudes and oscillation times. Oscillation time, T, and stop-start wave amplitude A from an idealized strongly periodic shape derived for the stop-start waves reported in Figures 5.9a,b and 5.9c,d (Kühne 1987) are as follows.

oscillation time T	16 min	15 min	7.5 min	5 min
amplitude A	70 km/h	70 km/h	40 km/h	25km/h
measurement figure	2 a	2 b	3 a	3 b

The data for Figures 5.9 a,b and 5.9 c,d are from the Institute of Transport Studies at the University of Karlsruhe, Germany (Michalopoulos and Pisharody 1980). The data above shows a proportionality between amplitude and oscillation time. This strong dependence is an expression for the non-linear and inharmonic character of the stop-start waves. In the case of harmonic oscillations, the amplitude is independent of the oscillation time as the linear pendulum shows. Obviously, the proportionality holds only for the range between traffic flow at a critical lane speed of about 80 km/h (= speed corresponding to the critical density $k_c \approx 25$ veh/km) and creeping with jam speed of about 10 km/h. For oscillations covering the whole range between free-flow speed and complete deadlock, saturation effects will reduce the proportionality.

As an example of transient effects, measurements from the Netherlands are described. The data are recorded as one-minute

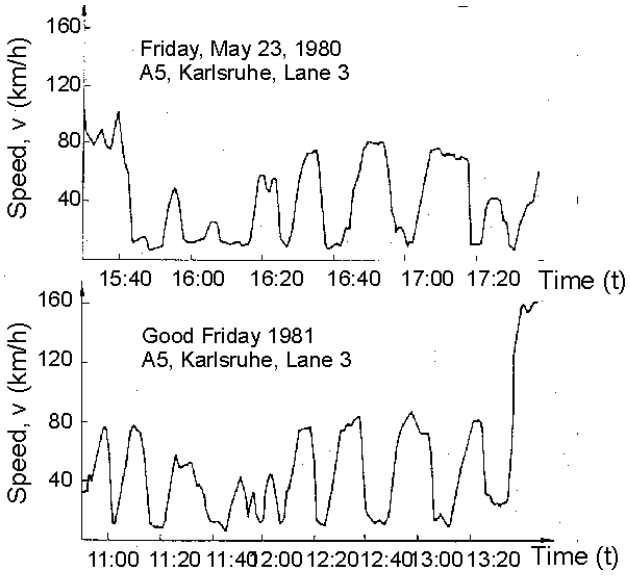

Figure 5.9 a,b
Time Series of Mean Speed for Unstable Traffic Flow (Michalopoulos and Pisharody 1980).

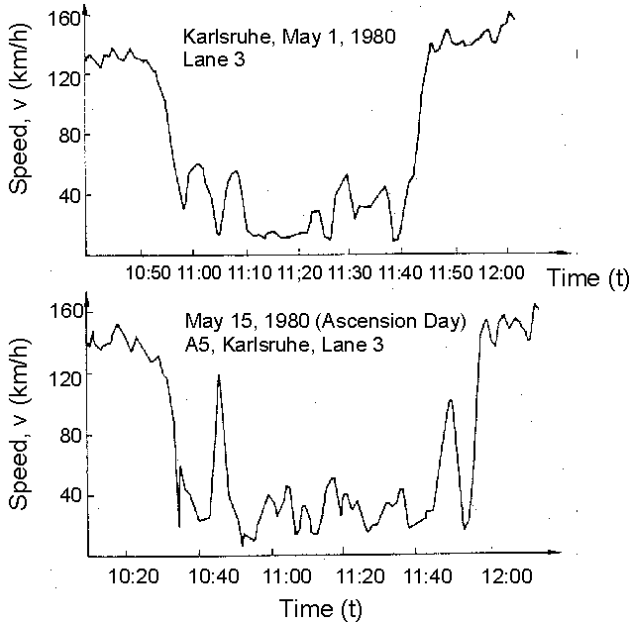

Figure 5.9 c,d
Time Series of Mean Speed for Unstable Traffic Flow with Small Undulations (Michalopoulos and Pisharody 1980).

Note: Data from the Institute of Transport Studies at the University of Karlsruhe, Germany.

average values from March 30, 1983 for the freeway A16 Westbound 1.1 to 4.35 km between 3:30 and 6:00 p.m. The section contains an auxiliary on ramp between 2.0 and 2.5 km and an exit to Rotterdam Centrum between 2.9 and 3.3 km, as well as, an entrance from Rotterdam Centrum between 3.8 and 4.35 km. The motorway is a three-lane highwaywith the exception between 3.3 and 3.8 km where the highwayhas only two lanes. Data are taken from measurement sites at 1.1, 1.6, 2.0, 2.5, 2.9, 3.3, 3.8, and 4.35 km which corresponds an average spacing of 500 m between each measurement site. In Figure 5.10, the one-minute mean values are plotted as a sequence of adjacent measurement sites. Figure 5.10 represents the time development of mean speed from adjacent measurement sites taken from the freeway A16 near Rotterdam, the Netherlands. The transient break in runs into stationary stop-start waves with amplitude ≈ 30 km/h and oscillation time ≈ 4 minutes. The traffic breakdown runs backwards with negative

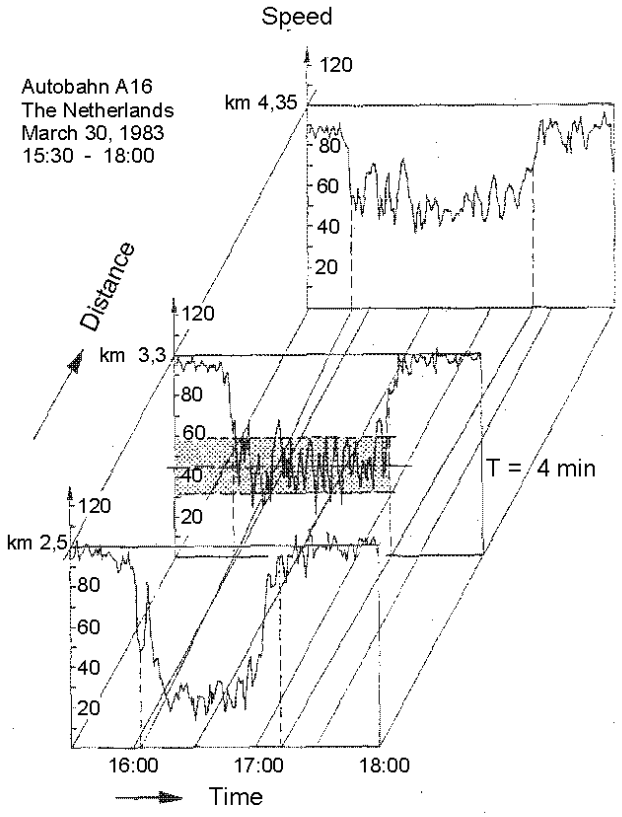

Figure 5.10
Time Development of Mean Speed from Adjacent Measurement Sites (Verweij 1985).

group velocity ≈ -10 km/h. Data from Verweij (1985). The data refers to the medium lane with almost only passenger car traffic.

The transient effects are very clear to recognize. At 4.35 km, there is a traffic breakdown from 3:50 to 5:20 p.m. with an average speed of 70 km/h compared to free flow speed of about 110 km/h. The speed development within the congested area is erratic with no marked oscillations. This breakdown is amplified from measurement site to measurement site upstream and becomes a regular stop-start wave at 3.3 km with an oscillation time of about four minutes and an amplitude of 30 km/h. At the far away upstream measurement site 1.1 km, due to wide spreading of the original disturbance, the traffic flow becomes erratic again where the area of slow traffic motion is almost completely damped out. The measurements also show that the traffic breakdown runs backwards with negative group velocity, so that upstream sites experience the breakdown later than downstream sites.

A number of comparable measurements exist. For instance, Koshi (Koshi et al. 1976) shows data from Tokyo expressway Radial Number 3. Again, the one-minute values show oscillations. At the beginning, and immediately after a weaving area which produces continuous disturbances, the oscillations are not very large in amplitude but are amplified as they propagate to the upstream. The highest waves reach a speed of approximately 40 km/h, and the oscillations of the two neighboring lanes of the regarded two-lane highwaybecome more synchronous as they propagate upstream. (See Figure 5.11.)

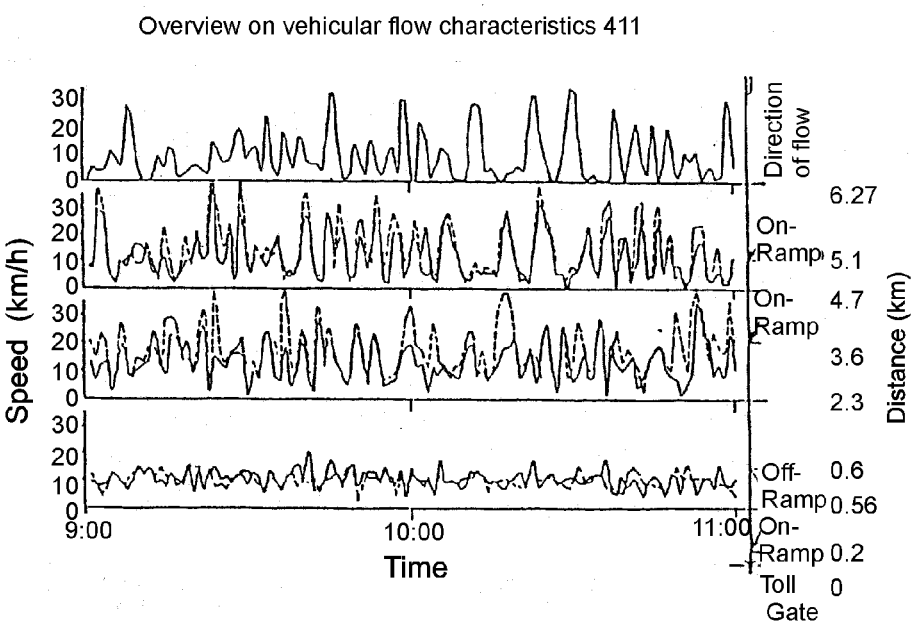

Note: _____: outer lane; -----: inner lane, average flow rate 1600 veh/h/2 lanes.

Figure 5.11
Time Development of Speed Upstream on Toll Gate at Tokyo Expressway (Koshi et al. 1976).

Other instructive measurement series for transients and stop-start waves are reported from Italy (Ferrari 1989). On the A14 near Bologna, data were collected on August 14, 1979 - the traditional summer exodus to holiday resorts with a number of long distance trips by drivers unaccustomed to using the motorway. This showed excellent examples of the formation of stop-start waves. For the U.S., comprehensive measurements over a long freeway stretch exist only for Interstate 80 between Oakland and San Jose, California. Usually, heavy loaded freeways are found within urban areas. There the distances between entrances and exits are short, usually ½ to 2 miles, which do not allow formation of stationary stop-start waves without being disturbed by merging traffic from extended weaving areas. The section between Hesperian and A-Street of the regarded stretch extend for 9000 ft; it has extremely good speed measurement equipment.

5.2.3 Momentum Equations

The extension of the simple continuum models in order to explain the dynamic effects in the preceding section was first pointed out by Whitham (1974) and Payne (1979). The actual speed *u(x, t)* of a small ensemble of vehicles is obtained from the equilibrium speed-density relation after a retardation time τ and from an anticipated location $x + \Delta x$:

$$u(x,t+\tau) = U_e(k(x+\Delta x,t)) \tag{5.41}$$

How to treat this recursive equation is shown in detail by Müller-Krumbhaar (1987). Expanding in a Taylor series with respect to τ and Δx - assuming both quantities can be kept small - yields to the substantial acceleration of a vehicle platoon

$$\frac{du}{dt} = \frac{1}{\tau}\left(U_e(k) - u\right) - c_0^2 \frac{k_x}{k} \tag{5.42}$$

where the arguments *x* and *t* are suppressed for convenience. In the right hand side of Equation 5.41, we used

$$\begin{aligned} U_e(k\ (x+\Delta x,t)) &= U_e(k) + \Delta x\ U_e'(k) k_x \\ &= U_e(k) - \tau c_0^2(k) \frac{k_x}{k} \end{aligned} \tag{5.43}$$

where $U_e'(k) < 0$. The derivative *dv/dt* is the acceleration of an observer moving along the streamline $x = x\ (t)$. In a fixed coordinate system this transforms into

$$\begin{aligned} \frac{du}{dt} = \frac{du(x(t),t)}{dt} &= u_x \frac{dx}{dt} + u_t \\ &= u_x u + u_t \end{aligned} \tag{5.44}$$

(i.e., the substantial acceleration is decomposed into a convection term indicating the acceleration due to spatial alterations of the stream lines, and into a local acceleration stemming from explicit time dependencies).

Continuity equation

$$k_t + (ku)_x = 0 \tag{5.45}$$

and momentum equation

$$u_t + u u_x = \frac{1}{\tau}\left(U_e(k) - u\right) - c_0^2 \frac{k_x}{k} \tag{5.46}$$

form a set of first order, partial differential equations which are supposed to describe dynamic effects associated with the traffic flow, such as stop-start waves formation, bifurcation into unstable flow and transients, and traffic behavior at bottlenecks. We mention, however, that basic equations cannot describe stop-start waves nor correct behavior at a bottleneck. Figure 5.12a shows speed measurements from Interstate 80 between Oakland and San Jose during morning peak with stop-start wave formation. Data for southbound shoulder lane after McCrank (1993) and Varaija et al. (1994). To interpret the different terms in the resulting momentum equation, a microscopic interpretation is given on the basis of a gas kinematic approach. It is assumed that a vehicular speed distribution function, *f(x,v,t)*, describes the number of *dN* of vehicles lying at time, *t*, on the road interval between x and $x + dx$ and having a speed between v and $v + dv$ by:

$$dN = f\ (x,v,t)\ dxdv \tag{5.47}$$

then the corresponding density increment is given by:

$$dk = f\ (x,v,t) dv \tag{5.48}$$

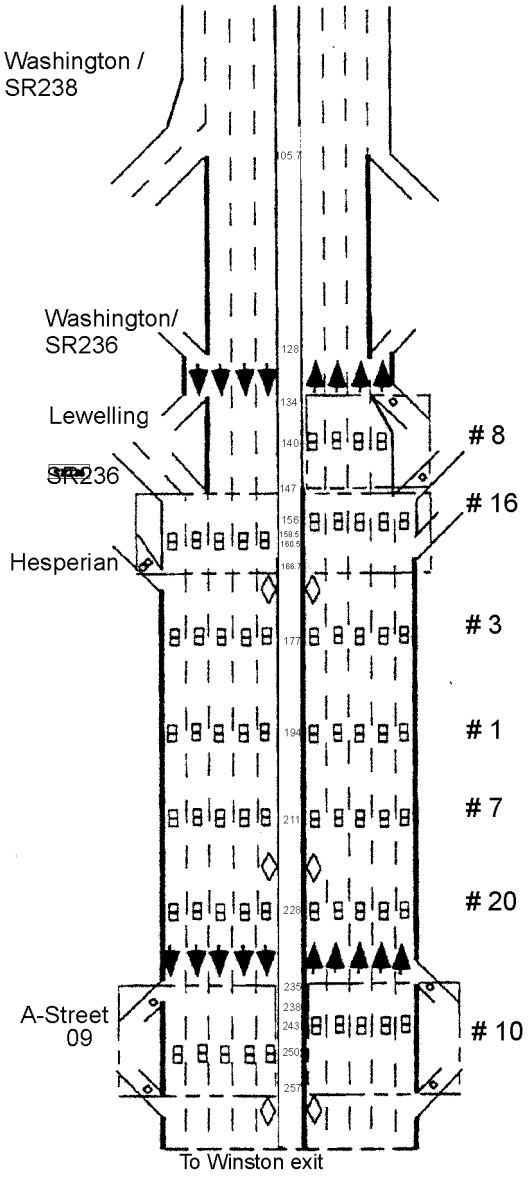

Note: Data for south bound shoulder lane during morning peak with stop-start formation after McCrank (1993) and Varaija et al. (1994).

Figure 5.12a
Speed Measurements from Interstate 80
between Oakland and San Jose.

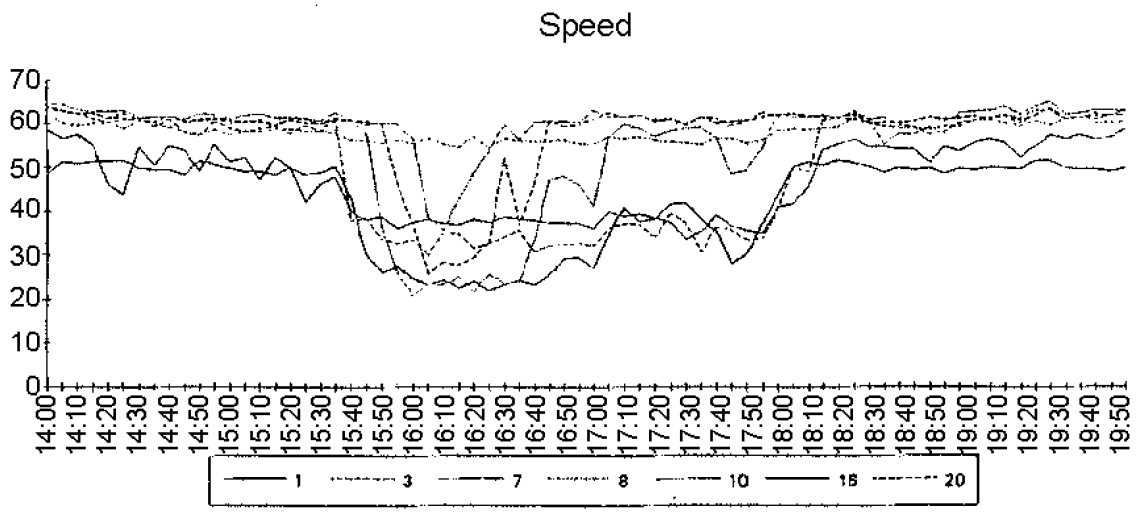

Figure 5.12b
Measurement Array for Speed Measurements from Interstate 80 between Oakland and San Jose after McCrank (1993) and Varaija et al. (1994).

while the density and mean speed are defined by:

$$k = \int_0^\infty f \quad (x,v,t)dv \tag{5.49}$$

$$u = \bar{v} = \int_0^\infty v\ f\ (x,v,t)dv\ /\int_0^\infty f\ (x,v,t)dv \tag{5.50}$$

Convection motion and relaxation to an equilibrium speed distribution f_o leads to an equation of motion for the distribution function f (Phillips and Prigogine 1979; Prigogine and Herman 1971) :

$$f_t + vf_x = \frac{1}{\tau}\left(f_0 - f \right) \tag{5.51}$$

Calculating the first and second moments of this equation of motion yields

$$k_t + (ku)_x = 0$$

$$(ku)_t + \partial_x \int v^2 f dv = \frac{1}{\tau}(Q(k) - q)_{q=ku} \tag{5.52}$$

Multiplying the momentum Equation 5.46 with k gives:

$$ku_t + kuu_x + c_0^2 k_x = \frac{1}{\tau}(Q(k) - q) \tag{5.53}$$

Upon comparing with (Equation 5.52), we finally obtain

$$c_0^2 k = \int_0^\infty (v^2 - u^2)\, f dv \tag{5.54}$$

The coefficient c_0^2 has therefore, the meaning of the standard deviation of the vehicular speed distribution. In kinematic gas theory, this speed distribution is linked to temperature. The gas kinematic interpretation can be completed by an interpretation stemming from sound propagation in compressible gases. Without relaxation and non-linear convection term, the continuity equation and momentum equation read

$$\begin{aligned} \frac{k_t}{k} + u\frac{k_x}{k} + u_x &= 0 \quad \Big| -c_0^2 \partial_x \\ u_t + uu_x + c_0^2 \frac{k_x}{k} &= \frac{1}{\tau}(U_e(k) - u) \quad \Big| \ \partial_t \end{aligned} \tag{5.55}$$

multiplied by $-c_0^2 \partial_x$ and ∂_t , respectively, gives

$$u_{tt} - c_0^2 u_{xx} = 0 \tag{5.56}$$

which is the sound propagation equation in compressible gases. The coefficient c_0^2, is therefore the sound velocity for propagation of disturbances without regarding non-linear convection and relaxation to equilibrium speed-density relation.

Finally, comparing the momentum equation with the hydrodynamic Navier Stokes equations

$$u_t + (u\nabla)u = -F + -\frac{1}{\rho}\nabla p + \frac{1}{\rho}\nabla\mu u$$

local acceleration + convection = volume force + pressure gradient + viscosity (5.57)

the term $-c_0^2 k_x / k$ can be identified with the traffic dynamic pressure

$$p = c_0^2 k \tag{5.58}$$

related to the potential of the traffic stream and the reversible part of the energy flow. These interpretations show that the pressure term $-c_0^2 k_x / k$ has the meaning of an anticipation term, which takes into account drivers´ reactions to downstream disturbances. As an approximation with limited application regimes

$$c_0^2 = \text{constant, independent of density } k \tag{5.59}$$

is used. A density dependence of the anticipation coefficient c_0^2 is investigated by Helbing (1994) as well as in the Section 5.2.9.

The relaxation term

$$\frac{1}{\tau}(U_e(k) - u) \tag{5.60}$$

describes the non-instantaneous adaption of the actual speed to the equilibrium speed-density relation. The relaxation time τ is the time a platoon of vehicles reacts to speed alterations. It has something to do with the reaction time of an ensemble of cars and must therefore be in the range of reaction time of drivers´ car-units

$$1s \lesssim \tau \lesssim 10s \tag{5.61}$$

For instance, the German "tachometer - half" rule fixes the legal safety distance, in meters, taking the half of the actual speed in km/h - leads to a reaction time of 1.8 sec as distance in meters during reaction leads to reaction time of 8 sec. It corresponds to the U.S. rule for every 10 mi/h, one more car length (old American passenger cars!).

Anticipating Section 5.2.10, again a value of τ = 1.8 sec indeed leads to excellent agreement between the model and calculations. Earlier papers (Cremer et al. 1993; Kühne 1991; Kühne 1984) have used much larger figures and interpret τ as a macroscopic reaction time which summarizes drivers´ reaction times. The use of unnatural high figures would lead to difficult interpretations (see e.g. Castillo, et al. 1993).

Relaxation and anticipation can be put together in a concise driving force term

$$\frac{1}{\tau}(U_e(k) - u) - c_0^2 \frac{k_x}{k} = \frac{1}{\tau k}(Q(k) - c_0^2 \tau k_x - q) \quad Q(k) = kU_e(k), \quad q = ku_e(k) \tag{5.62}$$

To anticipate drivers´ reactions, one substitutes the fundamental diagram $Q(k)$ by the volume-density relation $Q(k) - c_0^2 \tau k_x$

$$Q(k) \to Q(k) - c_0^2 \tau k_x \tag{5.63}$$

In view of this substitution, it becomes apparent that even under steady-state conditions maximum traffic volume is not constant but depends on the density gradient. In particular, it is interesting to note that it is allowed for q to become larger than q_{max}, namely if k is sufficiently high and, furthermore, k_x is negative.

For the equilibrium speed-density relation, $U_e(k)$, under homogeneous conditions several mathematical formulae have been proposed. A fairly general formula satisfying the boundary conditions:

- $U_e(k \to 0) \to u_f$
- $U_e(k \to k_{bumper}) \to 0$
- $U(k)$ *monotonic decreasing*. (5.64)

is given by (Cremer 1979),

$$U_e(k) = U_f\,(1-(k/k_{bumper})^{n_1})^{n_2} \tag{5.65}$$

with appropriate choice of the static parameters

$$\begin{aligned} U_f &= \text{free flow speed,} \\ k_{bumper} &= \text{density "bumper to bumper," and} \\ n_1, n_2 &= \text{exponents.} \end{aligned} \tag{5.66}$$

As a limiting case ($n_2 \to \infty$) the exponential functions

$$U_e(k) = u_f\, e^{-\frac{1}{2}(\frac{k}{k_{cr}})^2}, \; u_f\, e^{-\frac{k}{k_{cr}}} \tag{5.67}$$

can be used which do not approach zero at bumper to bumper density but which appeal by their simplicity.

Sometimes polynomial formulae are used such as

$$U_e(k) = \sum_{i=0}^{m} a_i\, k^i \tag{5.68}$$

or Padé polynomials

$$U_e(k) = \frac{\sum_{i=0}^{m} a_i\, k^i}{\sum_{i=0}^{n} b_i\, k^i} \tag{5.69}$$

The coefficients for all trials are determined from measurement points by the least squares method. The difficulty is to use only those points which refer to homogeneous and stationary situations and to cut off inhomogeneous nonstationary points. In (Dressler 1949) a self-consistent method is proposed to cut off unstable traffic flow situations. In all cases, one has to bear in mind that because the sample size for traffic includes only a few particles, fluid models have certain shortcomings which restrict their applicability in a strong mathematical sense.

5.2.4 Viscosity Models

Construction of stationary stop-start waves in the density regime beyond the stability limit can be done by introducing a collective coordinate

$$z = x - u_f\, t \tag{5.70}$$

which contains the unknown group velocity u_g. If density and mean speed depend only on the collective coordinate z

$$\begin{aligned} k(x,t) &= k(z) \\ u(x,t) &= u(z) \end{aligned} \tag{5.71}$$

the system of partial differential equations transforms into a system of ordinary differential equations. Then the basic equations read:

continuity equation

$$\{k(u-u_g)\}_z = 0 \tag{5.72}$$

and momentum equation

$$(u-u_g)u_z = \frac{1}{\tau}(U_e(k)-u) - c_0^2\frac{k_z}{k} \tag{5.73}$$

The continuity equation can be integrated immediately

$$k(u-u_g) = Q_0 \tag{5.74}$$

This means that the density and speed, in a frame running with group velocity u_g, must always serve as supplements. Wave solutions with a profile moving along the highway are only possible if the density at one site increases on the same proportion as the mean speed decreases with respect to the group velocity u_g and vice versa. The constant Q_0 has the meaning of a net flow and is a result of boundary and initial conditions to be fulfilled.

Substituting the integrated continuity equation into the momentum equation leads directly to a profile equation for speed profiles of stop-start wave solutions:

$$\left(\frac{u-u_g}{c_0} - \frac{c_0}{u-u_g}\right)U_z = \frac{1}{c_0\tau}\left(U_e\left(\frac{Q_0}{u-u_g}\right) - u\right) \tag{5.75}$$

To simplify the mathematical manipulations, dimensionless variables could be introduced

$$\frac{u-u_g}{c_0} = u' \qquad \frac{z}{c_0\tau} = z' \qquad \rho_0 = Q_0/c_0 \tag{5.76}$$

leading to the profile equation (' suppressed)

$$u_z = \frac{\frac{1}{c_0}U_e(\rho_0/u) - \frac{1}{c_0}u_g - u}{u - 1/u} \tag{5.77}$$

The profile equation, thus, is an ordinary differential equation of first order which can be directly integrated. It contains two arbitrary parameters: the flow rate $Q_0 \equiv \rho_0 c_0$ and the group velocity u_g.

The profile equation for u_z has a singularity. This singularity for vanishing denominator

$$u - 1/u = 0 \Rightarrow u = 1 \tag{5.78}$$

(negative speeds are excluded!)

has been discussed in detail by Dressler (1949). It is connected with vertical slope which can be either an inflection point or an extremum with respect to $z = z\,(u)$. An extremum would lead in a representation $u = u\,(z)$ to an ambiguous solution which has to be excluded. In order to get an inflection point, the conditions

$$\left.\frac{dz}{du}\right|_{pole} = 0 \qquad \left.\frac{d^2z}{du^2}\right|_{pole} = 0 \tag{5.79}$$

have to be fulfilled simultaneously. The calculations yield

$$\left.\frac{dz}{du}\right|_{pole} = \frac{u - 1/u}{\frac{1}{c_o}U_e(\rho_o/u) - \frac{1}{c_o}u_g - u} = 0 \quad \Rightarrow \quad u - 1/u = 0 \quad \frac{1}{c_0}U_e(\rho_0/u) - \frac{1}{c_0}u_g - u \neq 0 \tag{5.80}$$

$$\left.\frac{d^2z}{du^2}\right|_{pole} = \left.\frac{1 + 1/u^2}{\frac{1}{c_0}U_e(\rho_0/u) - \frac{1}{c_0}u_g - u}\right|_{pole} \neq 0 \tag{5.81}$$

and show that both conditions for an inflection point with vertical slope cannot be fulfilled simultaneously. The singularity has to therefore be cancelled, otherwise ambiguous solutions occur. In order to achieve this cancellation, the zeros of the denominator and numerator in the profile equation for u_z have to coincide which fixes the group velocity to

$$u_g = U_e(\rho_0) - c_0 \qquad \rho_0 \equiv Q_0/c_0 \tag{5.82}$$

Group velocity u_g and bottleneck capacity Q_0 are independent parameters; fixing their values to obtain unambiguous solutions indicates a limitation of the underlying model. With the values of the group velocity v_g and net flow rate Q_0 given by Equation 5.82, a monotonic shape of the profile is obtained, and so far no periodic solutions are available. This situation is identical to that of elementary shallow water theory, where the profile equations for a steady flow do not exhibit periodic solutions, although periodic roll waves are observed in every inclined open channel with suitable water height. To resolve this discrepancy, pieces of continuous solutions, as Figure 5.13 demonstrates, must be put together by jumps (Leutzbach 1985). To look for such partially continuous periodic solutions is an analogy to get shockwave formation within the kinematic wave theory. The dynamic theory provided up to now gives two reasons for a jumping solution. First, the starting point of the continuity equation is a conservation law for the vehicle number of a stretch; that is an integral law which allows finite jumps in the density. Secondly, the linear stability analysis developed in the subsequent section shows that higher wave numbers become more unstable than lower ones. This leads to a steeper shape of the speed and density profile and to the formation of shock fronts again containing finite jumps. To derive the jump condition, the profile equation is integrated over the discontinuity for an infinitesimal increment including the jump.

In hydrodynamics, integration is achieved by using higher order conservation laws like conservation of energy or of entropy. In traffic flow, such higher order conservation laws are not obvious and the derivation of jump conditions, therefore, is ambiguous. In connection with the correct selection of solutions of the kinematic wave theory, an entropy condition was formulated (Ansorge 1990; Bui et al. 1992)

$$\begin{aligned} &Q'(k_-) < \dot{x}_s(t) < Q'(k_+) \\ &\dot{x} \quad = \textit{shockspeed} \\ &k_-\,,\ k_+ \ = \textit{density downstream, upstream shock} \end{aligned} \tag{5.83}$$

The ambiguity can be resolved by using the experimental results:

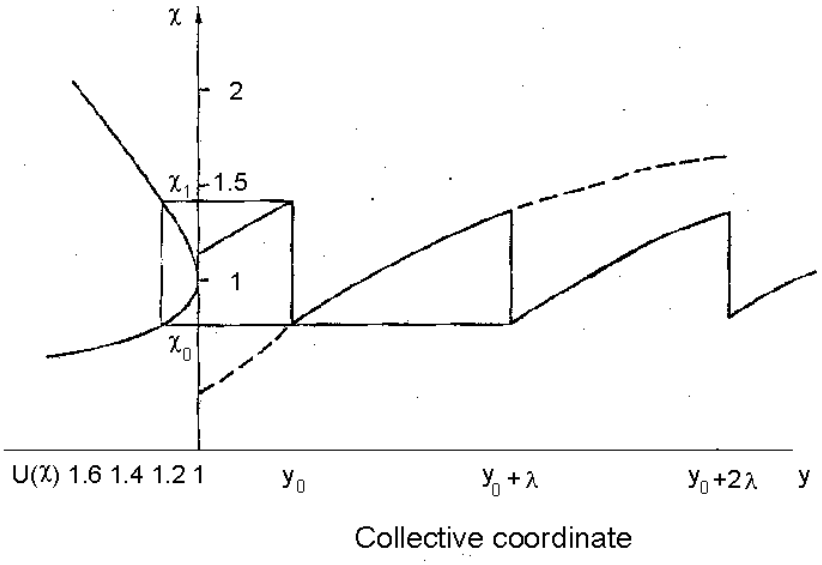

Figure 5.13
Construction of Partially Continuous Wave Solutions (Leutzbach 1985).

- the transition from free traffic flow (free flow speed 100-140 km/h Europe, 75 mi/h U.S.) to jammed-up traffic occurs on a length of minimum 80 m,
- the speed amplitude $A = u_{max} - u_{min}$ of a stop-start wave and the oscillation time, T, have the ratio $A/T \approx 280$ km/h^2 in the proportionality regime, and
- the group velocity for upstream running shock fronts in unstable traffic flow seldom exceeds $u_g = -20$ km/h. The experimental data suggest the presence of an intrinsic dampening that is modeled by introducing a viscosity term

$$\frac{1}{k}(\mu(k)u_x)_x$$

into the momentum equation. The basic higher order traffic flow model then reads:

$$k_t + (ku)_x = 0$$

$$u_t + uu_x = \frac{1}{\tau}\left(U_e(k) - u\right) - c_o^2\frac{k_x}{k} + \frac{1}{k}(\mu(k)u_x)_x \qquad (5.84)$$

The dynamic viscosity, μ_0, is determined by scaling investigations. In the shear layer, speed decreases from free flow to deadlock local acceleration, and dynamic viscosity overwhelms all other effects

$$u_t = \nu_0 u_{xx} \qquad \mu_0 = \frac{\nu(k)}{k} \quad \textit{approximately constant}$$

(*shear layer equation*) (5.85)

which leads to the speed profile within the shear layer decaying from free flow speed u_f to zero along the space coordinate x:

$$u \approx \frac{1}{\sqrt{4\pi\nu_0 t}}\, e^{-\frac{x^2}{4\nu_0 t}} \qquad (5.86)$$

and to the characteristic length l_0 during the characteristic time τ

$$l_0 = \sqrt{\nu_0 \tau} = \sqrt{\frac{\mu}{k}\tau}. \qquad (5.87)$$

There is minimal use of the viscosity model since its significance has not been completely understood. From the possible solutions of the kinematic theory, the entropy condition selects those which correspond to the lower envelope of the shock conditions (Bui et al. 1992). In the case of gas dynamics, this is very reasonable because it is well known that the Euler equations which display shocks are approximations of the Navier Stokes equations which contain viscosity and do not exhibit shocks.

As the numerical treatment later on shows a simple constant dynamic viscosity, $\mu(k)=\mu_0$ can be assumed which leads to the viscosity term μ. This approach is used constantly in the following

$$\text{viscosity term} = \frac{1}{k}\left(\mu(k)u_x\right)_x = \frac{\mu_0}{k}u_{xx}$$

The difficulties arising from the higher order models without viscosity (e.g. the inability to properly describe for bottleneck and stop-start behavior) are reviewed by Hauer and Hurdle (1979). The great numerical effort by Babcock et al. (1982) as well as the introduction of an adaptive discretization procedure by Cremer and May (1985) are attempts as well. From an analytical point of view, the latter procedures are nothing more than the introduction of a numerical viscosity in order to continuously describe bottleneck behavior and stop-start waves.

To obtain useful results, it is essential to overcome the mathematical problems of unphysical solutions due to vanishing viscosity by introducing the entropy condition or a small but not vanishing viscosity. Nevertheless, one has to keep in mind the limitations of the one-dimensional aggregate models presented (Papageorgiou 1989). In special traffic situations, the one-dimensional description fails. If an off-ramp throughput is less than the traffic wishing to exit, one or more right lanes of the main road may be blocked while traffic on the left lanes may be fluid. Restrictions of the one-dimensional description occur when trucks are not allowed to use the far left lane and block the right lane while traffic on the left lane may be fluid. Another restriction occurs if special lanes are dedicated to buses, taxis, and high occupancy vehicles.

5.2.5 Stability Analysis of Higher Order Models

The basic equations

$$\begin{aligned} k_t+(ku)_x &= 0 \\ u_t+uu_x &= \frac{1}{\tau}\left(U_e(k)-u\right)-c_o^2\frac{k_x}{k}+\frac{\mu_0}{k}u \end{aligned} \tag{5.88}$$

admit the equilibrium solution

$$k=k_0 \qquad v=U_e(k_0) \tag{5.89}$$

relying on the equilibrium speed-density relation $U_e(k)$. To determine the stability of this solution the trial solution

$$\begin{aligned} k &= k_0+\tilde{k}e^{ilx+\omega(l)t} \\ u &= U_e(k_0)+\tilde{u}e^{ilx+\omega(l)t} \end{aligned} \tag{5.90}$$

is substituted in the model equations and only term up to first order in $\tilde{k}$ and $\tilde{u}$ are considered (for convenience dimensionless coordinates

$$x' = \frac{x}{c_o\tau} \qquad t' = \frac{t}{\tau}$$

are used where ' is suppressed). In Equation 5.90, l is the wave number and ω (l) is the corresponding frequency.

The continuity and the momentum equations are rewritten as:

$$\begin{aligned} &\left(\omega+il\frac{1}{c_0}U_e(k_0)\right)\tilde{k}+ilk_0\tilde{u} = 0 \\ &\left(\omega+il\frac{1}{c_0}U_e(k_0)\right)\tilde{u} = \frac{1}{c_0}U_e'(k_0)\,\tilde{k}-\tilde{u}-il\,\frac{1}{k_0}\,\tilde{k}-\nu l^2\tilde{u} \end{aligned} \tag{5.91}$$

with ν as the inverse Reynolds number

$$\nu=\frac{\mu_o}{k_o^2\tau} = \frac{1}{Re} \tag{5.92}$$

The condition for non-trivial solutions yields the eigenvalues

$$\omega=il\frac{1}{c_0}U_e(k_0)-\frac{1+\nu l^2}{2} \pm \sqrt{\left(il+\frac{1+\nu l^2}{2}\right)^2 + il(a-\nu l^2)} \tag{5.93}$$

where a is the dimensionless traffic parameter

$$a=-1-\frac{k_0}{c_0}\,U_e'(k_0). \tag{5.94}$$

The traffic parameter characterizes the traffic conditions by increment of speed density relation and absolute value of the operating point k_0. Regarding only the infinitesimal vicinity of the operating point corresponds to the restriction on a linear stability analysis and is similar to the wave theoretic stability interpretations in kinematic traffic wave theory.

The two branches of the eigenvalues correspond to two different types of excitations. One branch leads to permanent negative real part (- sign) and is, therefore, stable. The other branch (+ sign) has a real part which can change its sign independent of the traffic parameter a and which then leads to instability of the equilibrium solution. The cross-over point is given by

$$l^2 = a/\nu. \tag{5.95}$$

This corresponds to a real wave number if $a > 0$, which becomes a necessary condition for unstability. For $a < 0$, no cross over point can be reached. The overall stability analysis is stable $a <$ 0 equilibrium for solution can become unstable $a > 0$ was also derived by Payne (1979).

The wave number dependence on the real part of the eigenvalue ω together with the stability domain is shown in Figure 5.14 and Figure 5.15. Figure 5.14 shows the wave number dependence of the real part of the eigen values for $a > 0$ from the linear stability analysis of the equilibrium solution (Kühne and Beckschulte 1993). The positive values of the upper branch lead to instability of the equilibrium solution.

The corresponding eigenfunctions can easily be calculated to

$$\begin{pmatrix} k \\ u \end{pmatrix} = \begin{pmatrix} k_0 \\ U_e(k_0) \end{pmatrix} + N \begin{pmatrix} -ilk_0 \\ (\omega(l) + il\ U_e(k_0)) \end{pmatrix} e^{ilx+\omega(l)t} + c.c. \tag{5.96}$$

where N is a normalization constant. For instance at the transition point

$$l = l_c = \sqrt{a/\nu}$$

the upper branch reads

$$\begin{pmatrix} \frac{k}{k_0} \\ \frac{u}{c_0} \end{pmatrix} = \begin{pmatrix} 1 \\ \frac{1}{c_0} U_e(k_0) \end{pmatrix} + N \begin{pmatrix} -il_c \\ il_c \end{pmatrix} e^{il_c\left(x - \frac{U_e(k_0)}{c_0}t + t\right)} + c.c. \tag{5.97}$$

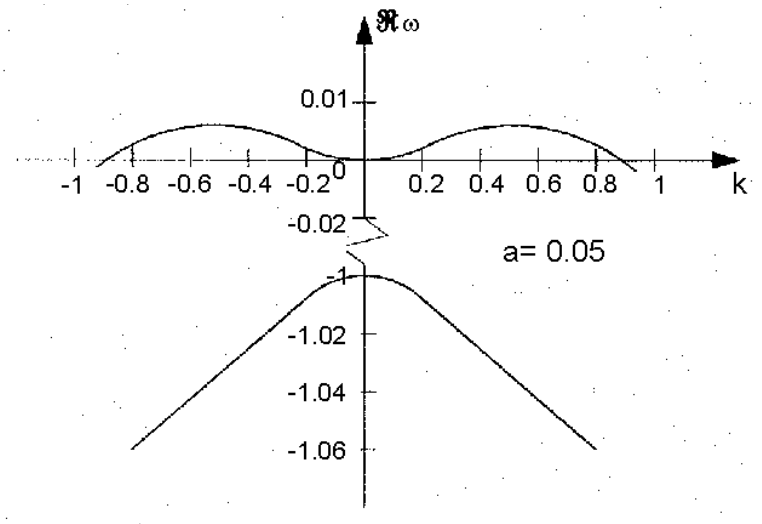

Figure 5.14
Wave Number Dependence from the Linear Stability Analysis.

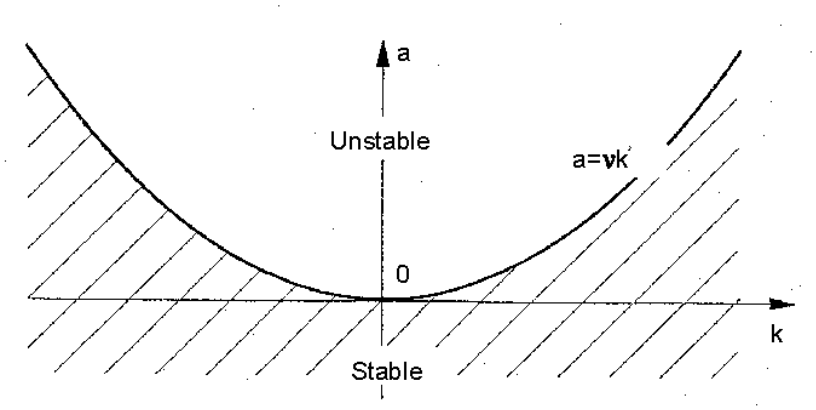

Figure 5.15
Traffic Parameter a and Stability Domain of the Homogeneous Traffic Flow.

To interpret this upper unstable branch, the sign of density and speed deviations from the equilibrium are considered the upper branch describes excitations where speed and density vary in opposite direction. A speed increase with respect to the homogeneous equilibrium solution $k = k_0$, $u = {}_e U_0(k)$ corresponds to a decrease of density. This excitation leads to unstable traffic flow beyond a critical density. If it is possible to react throughout the whole excitation by modulations of speed and density which go in phase, the second and lower branch is reached which leads to stable but unnatural behavior in traffic engineering. The drivers´ reaction to reduce the speed in heavy traffic flow when density is increasing is the reason for instabilities, spreading of shock waves, and formation of congestion with stop-start waves. Of course, this reaction is correct with respect to safety. With artificial distance control systems, however, the lower branch excitation becomes feasible. The reaction "higher density - higher speed" then leads to the expected increase of capacity by means of distance control systems.

In the unstable regime, the linear stability analysis indicates exponential growing of perturbances. Since, saturation effects will confine the increase of a non-linear stability, analysis in the unstable regime has to be considered. Several methods of non-linear stability analysis have been developed to describe the correct behavior in the unstable regime, mostly based on a truncated expansion using the eigenmode expansion from linear stability analysis as a starting point. Under certain circumstances chaotic motion is observed by this complete analysis, (i.e., the unstable traffic patterns are connected with non-linearity stochastics) (Kühne and Beckschulte 1993). These non-linearity stochastics define time and length scales of coherence which have to be distinguished from ordinary noise due to omnipresent random influences.

5.2.6 Numerical Solutions by Finite Element Method

Over a wide range, higher order models up to now have failed to demonstrate their superiority over simple continuum models even after improving the solution algorithms. This situation is similar to the application of the Euler equations in hydrodynamics in comparison with simple hydrostatic considerations, which do not yield improved results and even yield wrong results (e.g., shear layers, buoyancy, and boundary conditions for eddies). The full fluid dynamic effects can be taken into account correctly only at the Navier Stokes level. It is, therefore, no surprise that traffic flow at bottlenecks, formation of stop-start waves, and the variety of traffic patterns in unstable traffic flow could only be described with higher order models (including viscosity and differentiating between vanishing viscosity and viscosity tending to zero). Besides the in-depth understanding of the macroscopic traffic flow mechanisms, appropriate numerical methods have to be provided. Simple forward discretization schemes are not

suitable and in many cases lead to wrong results due to the connected numerical instabilities.

The numerical methods must contain:

- Implicit integration procedures with centered differences and correct treatment of the non-linearities by a Newtonian iteration procedure, which is stable under all conditions and
- Correct recording of boundary and initial conditions regarding the hyperbolic character of the basic differential equation system.

The implicit procedure turns out to be numerically stable if the coefficients do not alter suddenly. Bottlenecks have therefore to be introduced with smoothed boundaries.

Sometimes additional simplifications can be used (e.g., using logarithmic density or separating the conservative part of the momentum equation); these methods are linked to special forms of an anticipation term and a fundamental diagram which cannot be recommended in general.

Crucial for the numerical solution is the correct choice of the spatial and temporal step size for discretization of the space and time coordinate. A number of papers propose a spatial step size of about 500 m arguing that this is the coherence length of spatial variations and is traditionally equal to the spacing of measurement sites (e.g. dense equipped line control systems or tunnel stretches) (Cremer 1979). Experience with numerical solutions shows that significantly smaller sizes have to be considered. The calculations concerning the Boulevard Périphérique around Paris use 125 m and propose even smaller discretization structures (Papageorgiou et al. 1990). The smaller structure is induced by the characteristic length of shear layers (l_o = 80 m) and is motivated by the minimum size of variations which coincide with one car length. Since the numerical effort is inconsiderable,

$$\Delta x = 5\ m \tag{5.98}$$

will be chosen throughout numerical procedures.

The spatial step size is connected via the characteristic speed with the temporal step size. As appropriate, the backward propagation speed of shock waves of about 20 km/h is chosen in order to also record shock front spreading. This gives

$$\Delta t = 1\ \text{sec} \tag{5.99}$$

Since the time step is smaller than the usual actualization rate of measurements for boundary conditions (which usually come in a 30 sec scanning rate), the measurement data have to be interpolated providing a smoothing effect welcome for stabilizing the numerical calculations.

For numerical integration, the basic equations are transformed by

$$u_x = w \tag{5.100}$$

into a system of three equations for the unknown variables k, v, and w. To identify the static and dynamic parameters at one glance, the variables are normalized in the following way:

$$k' = \frac{k}{k_{ref}} \qquad u' = \frac{u}{u_f} \qquad w' = \frac{w}{u_f} \qquad x' = \frac{x}{u_f \tau} \qquad t' = \frac{t}{\tau} \tag{5.101}$$

where the reference state k_{ref} can be the density bumper to bumper in case of a unique lane number. The unknown variables can be put together to a vector η,

$$\eta = \begin{pmatrix} k \\ u \\ w \end{pmatrix} \tag{5.102}$$

and the basic equations have the form of a quasi-linear partial differential equation:

$$A\eta_t + B\eta_x = C \tag{5.103}$$

with

$$A = \begin{pmatrix} 1 & 0 & 0 \\ 0 & 1 & 0 \\ 0 & 0 & 0 \end{pmatrix} \quad B = \begin{pmatrix} u & 0 & 0 \\ \frac{1}{k}\frac{1}{Fr} & 0 & \frac{1}{Re} \\ 0 & 1 & 0 \end{pmatrix} \quad C = \begin{pmatrix} & -kw & \\ -uw & +U & -u \\ & w & \end{pmatrix} \tag{5.104}$$

The equations contain the static speed-density fit,

$$U_e(k) = \left(1 - \left(\frac{k_{ref}}{k_{bump}(x)} k \right)^{n_1} \right)^{n_2} \tag{5.105}$$

with the exponents n_1 and n_2 describing the density dependence, as well as with the density "bumper to bumper," $k_{bump}(x)$, which is space-dependent in the case of lane dropping and bottlenecks.

The basic equations contain two dynamic parameters:

$$Froude\ number = \frac{kinetic\ energy\ (inertia\ influence)}{potential\ energy\ (pressure)} = \frac{\left(\frac{1}{2}\right) k u_f^2}{c_0^2 k} = \left(\frac{u_f}{c_0} \right)^2 \equiv Fr$$

$$Reynolds\ number = \frac{length\ velocity}{kinem.\ viscosity} = \frac{u_f^2 \tau}{\nu_0} \equiv R \tag{5.106}$$

We integrate Equation 5.103 along its characteristics. To ensure uniqueness, we need two initial conditions, e.g.

$k = k\ (x,\ t = 0)$ $\quad u = u\ (x,\ t = 0)$ and

three boundary conditions, e.g.,

$$k = k\ (x = 0,\ t) \quad u = u\ (x = 0,\ t) \quad w = w\ (x = 0,\ t) \tag{5.107}$$

For numerical stable solutions, the hyperbolic character of the differential equation system has to be considered. Therefore, only few boundary conditions on the left and right boundary can be used:

$$k = k\ (x = 0,\ t) \quad u = u\ (x = L,\ t) \quad u = u\ (x = 0,\ t) \tag{5.108}$$

For detailed numerical solution, the equations are integrated section wise according to the scheme shown in Figure 5.16 (Kerner and Konhäuser 1993a).

To this aim the continuous functions,

$$\eta(x,t) = \begin{pmatrix} k & (x,t) \\ u & (x,t) \\ w & (x,t) \end{pmatrix} \tag{5.109}$$

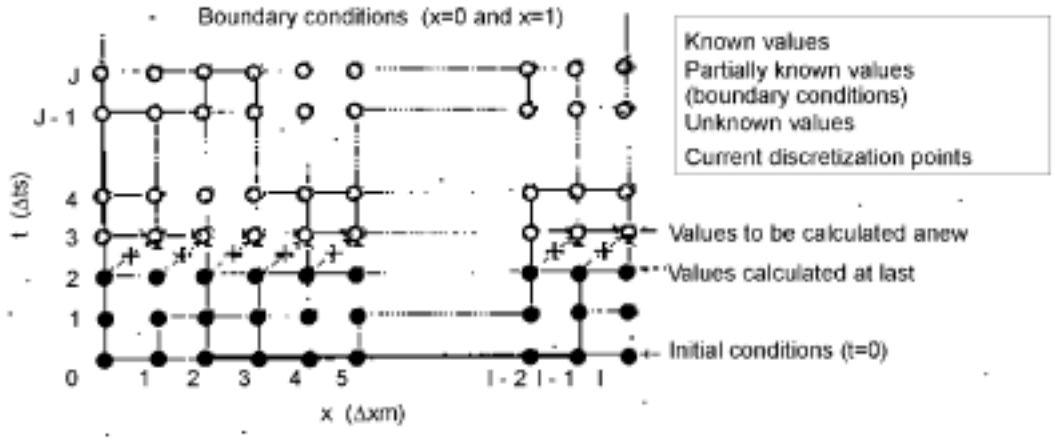

Figure 5.16
Stepwise Integration of the Quasi Linear Differential Equation in Time and Space Grid (Kerner and Konhäuser 1993a).

are replaced by functions defined as a lattice:

$$\eta(x_0+i\Delta x, t_0+j\Delta t) \equiv \eta_{i,j} \tag{5.110}$$

All derivatives are replaced by centered difference quotients

$$\eta_x \rightarrow \frac{1}{2\Delta x}\left(\eta_{i+1,j+1} - \eta_{i,j+1} + \eta_{i+1,j} - \eta_{i,j}\right) \tag{5.111}$$

$$\eta_t \rightarrow \frac{1}{2\Delta t}\left(\eta_{i+1,j+1} + \eta_{i,j+1} - \eta_{i+1,j} - \eta_{i,j}\right) \tag{5.112}$$

and the function values are replaced by the midpoint values

$$\eta \rightarrow \frac{1}{4}\left(\eta_{i+1,j+1} + \eta_{i,j+1} + \eta_{i+1,j} + \eta_{i,j}\right). \tag{5.113}$$

The integration procedure is a stepwise process starting with the variable at the known time layer $t = t_0+\Delta t \cdot j$,

$$\eta_{i,j}$$

known variables to start with

$$\eta_{i+1,j} \tag{5.114}$$

and proceeding from this layer to the next unknown layer $t = t_0+\Delta t \cdot (j+1)$

$$\eta_{i,j+1} \equiv \eta_i$$

unknown variables to be calculated

$$\eta_{i+1,j+1} \equiv \eta_{i+1} \tag{5.115}$$

Since the basic equation are non-linear, an implicit procedure must be used with respect to the unknown variables η_i, η_{i+1}. It turns out that the Newtonian iteration procedure is extremely stable. The variables are replaced by an approximation $\bar{\eta}_i$, $\bar{\eta}_{i+1}$ and the deviations $\delta\eta_i$, $\delta\eta_{i+1}$ are calculated by linearizing the starting equations. Denoting the deviation vector by:

$$\delta_i \equiv \begin{pmatrix} \delta k_i \\ \delta u_i \\ \delta w_i \end{pmatrix} \tag{5.116}$$

the basic equations can be written in the form of

$$A_i\delta_{i+1}+B_i\delta_i = R_i \tag{5.117}$$

with $$\left(\alpha=\frac{2}{\Delta x},\ \beta=\frac{2}{\Delta t},\ \kappa=\frac{1}{Fr}=\frac{c_0^2}{v_f^2}\right) \tag{5.118}$$

$$A_i=\begin{pmatrix} \beta+\alpha U+W & K_x & K \\ -U_e'(K)-\kappa\frac{K_x}{K^2}+\alpha\kappa\frac{1}{K} & \beta+W+1 & U-\alpha v \\ 0 & \alpha & -1 \end{pmatrix} \tag{5.119}$$

$$B_i=\begin{pmatrix} \beta-\alpha U+W & K_x & K \\ -U_e'(K)-\kappa\frac{K_x}{K^2}-\alpha\kappa\frac{1}{K} & \beta+W+1 & U+\alpha v \\ 0 & \alpha & -1 \end{pmatrix} \tag{5.120}$$

$$R_i=-4\begin{pmatrix} K_t + K_xU + K \\ U_t+UW-U_e(K)+U+\kappa\frac{K_x}{K}-vW_x \\ U_x - W \end{pmatrix} \tag{5.121}$$

where the abbreviations

$$K = \frac{1}{4}\left(\bar{k}_{i+1} + \bar{k}_i + k_{i+1,j} + k_{i,j}\right) \tag{5.122}$$

$$K_t = \frac{1}{2\Delta t}\left(\bar{k}_{i+1} + \bar{k}_i - k_{i+1,j} - k_{i,j}\right) \tag{5.123}$$

are used.

Starting with the initial condition as the lowest approximation,

$$\bar{\eta}_i = \eta_{i,j=0} \quad \eta_{i,-1} = 0 \tag{5.124}$$

and using the left boundary condition,

$$\begin{matrix} k_{i=0,j} \\ V_{i=0,j} \end{matrix} \Rightarrow \delta_0 = \begin{pmatrix} 0 \\ 0 \\ \delta w_0 \end{pmatrix} \tag{5.125}$$

the δ_i are calculated recursively by

$$\delta_{i+1} = A_i^{-1}\left(R_i - B_i\delta_i\right) \tag{5.126}$$

as a function of δw_0 , which in turn is determined by the right boundary condition

$$v_{i=I,\,j} \Rightarrow \delta_I = \begin{pmatrix} \delta k_I \\ 0 \\ \delta w_I \end{pmatrix} \tag{5.127}$$

An alternative rearrangement of the deviations δ_i is possible in order to produce a tridiagonal form which facilitates the fit of the boundary conditions (Kerner and Konhäuser 1993a).

The complete numerical solution procedure is shown in the flow chart of Figure 5.17.

5.2.7 Parameter Validation with Examples from Actual Measurements

For parameter validation, we compare measurements at an intermediate cross-section with calculations of mean speed and traffic volume or local density based on the model under investigation. The principle is shown in Figure 5.18.

Mean speed and traffic volume or local density are measured at the boundaries $x = 0$ and $x = L$ and at the intermediate distance $x = d$. The initial condition is mainly a uniform distribution compatible with the boundary condition series. After some transient iterations, the course of mean speed and local density is calculated from the model equations and compared with the intermediate measurement.

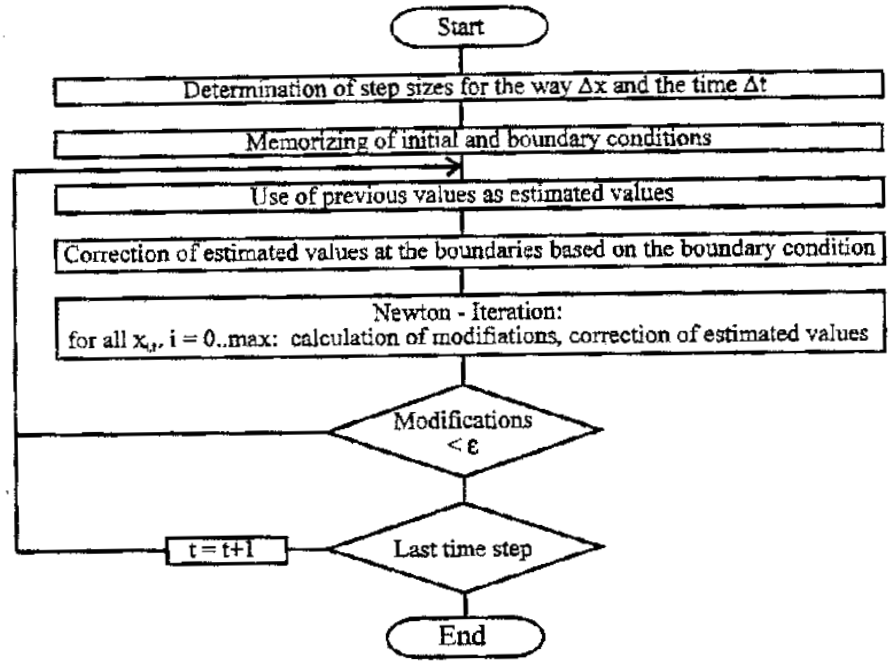

Figure 5.17
Flow Chart of the Numerical Solution Procedure (Kerner and Konhäuser 1993a).

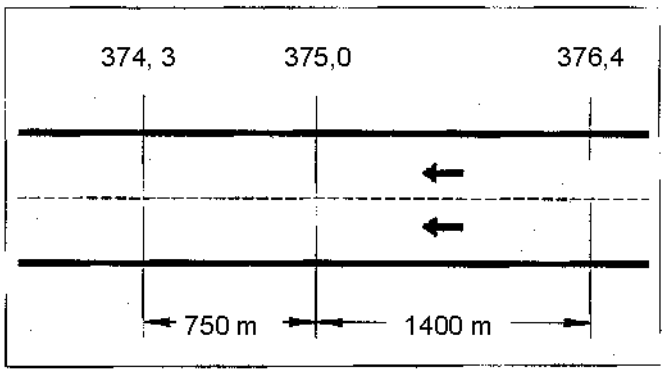

Figure 5.18
Principal Arrangement for Parameter Validation
by Comparison of Measurements and Calculations.

The performance index, defined as

$$PI = \gamma_1 \int dt \left(u_{cal.}(d,t) - u_{meas.}(d,t)\right)^2 + \gamma_2 \int dt \left(k_{cal.}(d,t) - k_{meas.}(d,t)\right)^2 \qquad (5.128)$$

is a function of the static and is to be minimized,

$$PI = PI\left(v_f,\ k_{bump},\ n_1,\ n_2,\ d_0,\ v_0\right) = Min \qquad (5.129)$$

by the optimal parameters.

Obviously, the results depend on the step sizes chosen in the discretization procedure. Step sizes together with static and dynamic parameters form a set of at least eight parameters which have to be chosen simultaneously to achieve minimum. Systematic procedures like minimum determination by gradient method or comparable methods appear to be too complicated. Instead, Monte Carlo methods reduce the computational effort and give reasonable results. In some approaches (Babcock et al. 1982), the static speed-density relation is calibrated individually for each subsection. In the validation procedure described here, the model is calibrated with a unique speed-density characteristic. This is based on data from the follow-up versions of the Highway Capacity Manual (HCM) (Wemple et al. 1991), including data from Europe and the U.S. One main reason to redesign the high flexibility in matching the real observations for each subsection individually is the lack of sufficient data. The unique speed-density characteristic depends on geometrical data (number of lanes, slope, curvature) and environmental conditions (weather, time of day), rather than on the specific location. Speed limits are introduced by reducing the free flow speed and the exponents n_1, n_2 in case of an analytical relation which uses powers (Cremer 1979) (an example is given in the following). Different truck ratios can be introduced by altering the density bumper to bumper for which the transformation

$$\frac{1}{k_{bump}} = f\frac{1}{k_{pass.}} + (1-f)\frac{1}{k_{truck}} \qquad (5.130)$$

f = relative truck portion, $k_{pass} = k$
k_{pass} = density "bumper to bumper" for 100% passenger cars
k_{truck} = density "bumper to bumper" for 100% trucks

is appropriate.

For validation, data from the Autobahn A3 Fürth-Erlangen near Nuremberg are used. It is within a line control system with corresponding dense measurement cross sections approximately every 1,000 m. Between the access Frauenaurach and Erlangen-West in the direction of Frankfurt a.M., six cross sections with 980 m average spacing are available every 60 sec. The data are near values, separately detected for passenger cars and the rest of the vehicles (discriminated by vehicle length) for each lane of the two-lane carriageway. A stretch was selected with a total length of 2,100 m with left-hand side and right-hand side boundary conditions and an intermediate cross section which is 1,400 m apart from the left boundary.

Data were taken during the weekend of November 7 and 8, 1992 with a relatively low truck ratio. With the Monte Carlo method, the following parameters were selected for a two-lane highway

$$\begin{aligned} u_f &= 140 \text{ km/h} \quad & k_{bump} &= 350 \text{ veh/km} \\ n_1 &= 1.4 & n_2 &= 4.0 \\ c_o &= 70 \text{ km/h} & \tau &= 1.8s \quad \nu_o = 12.8 \text{ km}^2/\text{h} \end{aligned} \tag{5.131}$$

Figure 5.20 shows the time series of the mean speed at the intermediate cross section together with the simulated data. The course is reproduced by the simulation in detail, while the strong elongations are slightly smoothed.

The corresponding dimensionless numbers are:

$$\begin{aligned} Fr &= \left(\frac{v_f}{c_0} \right)^2 = 4.0 \\ Re &= \frac{v_f^2 \tau}{\nu_0} = 0.77 \end{aligned} \tag{5.132}$$

It turns out that the traffic flow model describes a fluid in the intermediate state between low and high Reynolds numbers. Since it is now a high Reynolds number fluid, a neglection of the viscosity term is not possible. An expansion with respect to small Reynolds numbers is not possible.

The shear layer depth is

$$l_o = \sqrt{\nu_o \tau} = 80m \tag{5.133}$$

and the critical density for the two-lane highwayis calculated from

$$a = -1 - \frac{k_c}{c_0} \frac{dU_e(k_c)}{dk} = 0 \tag{5.134}$$

to

$$k_c = 50 \; veh/km \left(\frac{k_c}{k_{bump}} \right)^{1.4} = 0{,}3863 \tag{5.135}$$

Another European example, data from French freeways are taken. The Boulevard Périphérique as the ring freeway around Paris is well-equipped with measurement stations. Since there is a general speed limit on French freeways, the data differ from German Autobahn data. Figure 5.19 shows the arrangement of the measurement cross sections. Figure 5.20 reproduces the time series of traffic volume and mean speed from the measurement sites which serve as basic data.

For a further detailed investigation in parameter validation, the reader is referred to three comprehensive examples:

(1) A3 Fürth-Erlangen near Nuremberg, Germany (see Kühne and Langbein- Euchner 1993),

(2) Boulevard Périphérique, Paris, France (see Papageorgiou et al. 1990), and

(3) Interstate 35 W in Minneapolis, MN (see Sailer 1996).

5.2.8 Calculation of Traffic Flow at a Bottleneck

The calculation of traffic behavior at a bottleneck turns out to be the crucial test for the usefulness of a traffic flow model. The observations of traffic flow at a bottleneck are:

- Traffic volume can exceed capacity within the bottleneck only for a short time maximum of some minutes;
- Traffic density can at no point exceed density bumper to bumper;
- If travel demand exceeds capacity, congestion occurs in front of the bottleneck location;
- Spilled-up traffic is marked by upstream running shock fronts and the formation of stop-start waves in the congested regime;
- Spatial changes occur on scales shorter than 100 m; and
- The boundary conditions have to be chosen in such a way that traffic patterns and resulting traffic volume are effects of and not causes for traffic dynamics.

A reduction of lanes (two-lane to one-lane) has been simulated on the basis of the previously described high order macroscopic traffic flow model.

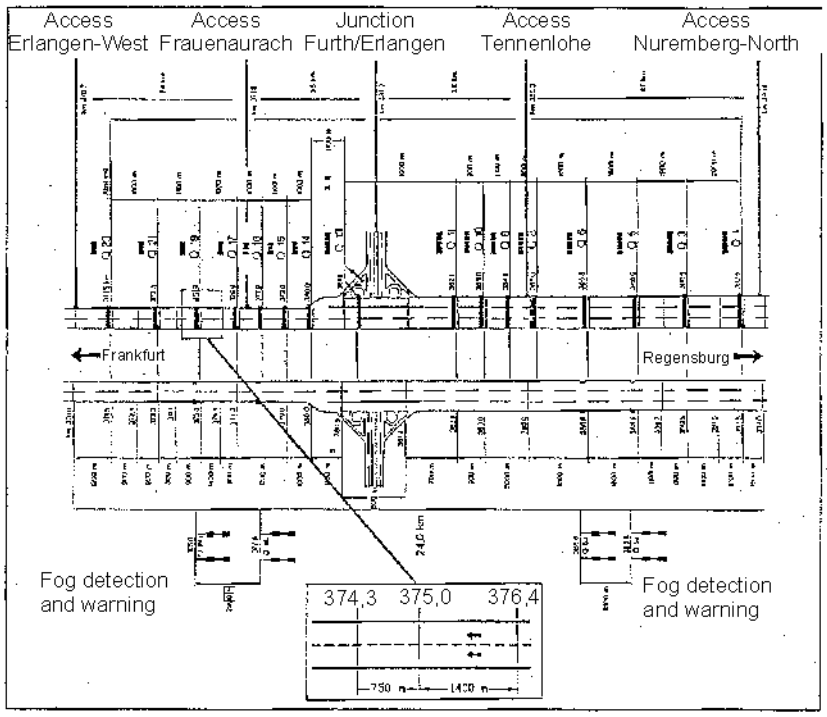

Figure 5.19
Autobahn Section for Validation of the Macroscopic Freeway Model.

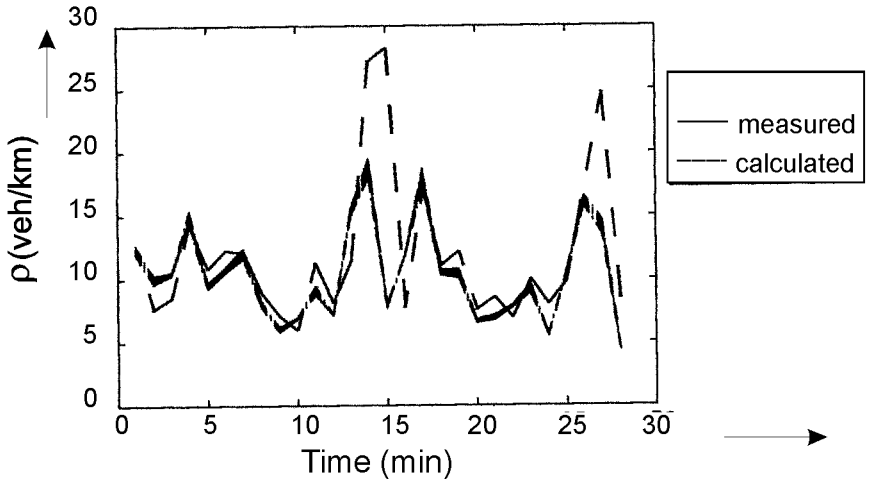

Figure 5.20
Measurement and Simulated Time Series at the Mean Speed of the Intermediate Cross Section on the Test Section.

The following results for a 10 km stretch of a two-lane highwayare shown with a bottleneck - reduction of maximum density from 320 to 220 vehicles per km - between the space marks of 6.5 and 8.5 km as shown in Figure 5.21a. Within the bottleneck a high density regime is formed. The minimum of the speed lies at the first third of the bottleneck. At the outlet, due to the metering effect of the bottleneck, speed increases and the calculations show clearly the corresponding rise.

From the minimum speed within the low speed regime, an overreaction of the drivers is deduced. This overreaction in braking forces an acceleration as revenge and thus leads - if the overall speed is sufficiently low - to an upstream movement of the speed minimum within the bottleneck. The beginning of the overreaction regime itself is spreading downstream and reaches finally the end of the bottleneck.

Figures 5.21b-d show the development of the speed course for a 1000 seconds time period; after an initially homogeneous constant distribution forms a spatial structure.

Figure 5.21b shows the temporal traffic speed development up to 200 seconds after an initially homogenous density distribution. This formation is accelerated by using boundary conditions for the left boundary, that put a higher value of traffic volume into the stretch. The speed course in Figure 5.21b shows the relaxation of this initially inhomogeneous flow to homogenous flow in the first part of the stretch. The bottleneck lasts from space mark 6500 m to 8500 m. Calculations are from Sailer. Figure 5.21c shows the traffic speed course after 300 to 800 seconds. The speed peak wanders upstream while the overreaction regime fades away. Additional undulations are formed - the stop-start waves. Figure 5.21d shows the traffic speed course at the bottleneck after 1000 seconds. In the congested area, in front of the bottleneck well established stop-start waves occur.

The first group from the series of snap shots reproduce the formation of a density peak within the bottleneck. The second group indicates the movement of the density peak on the one

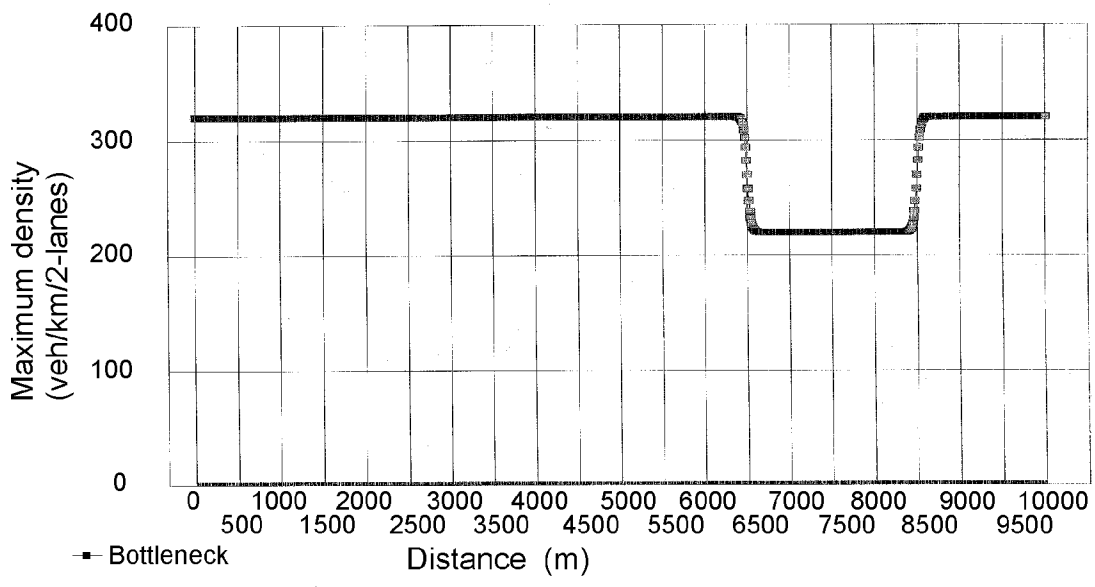

Note: Immediately after an initially homogeneous density distribution.

Figure 5.21a
Temporal Traffic Density Development One to Four Minutes (derived from Sailer 1996).

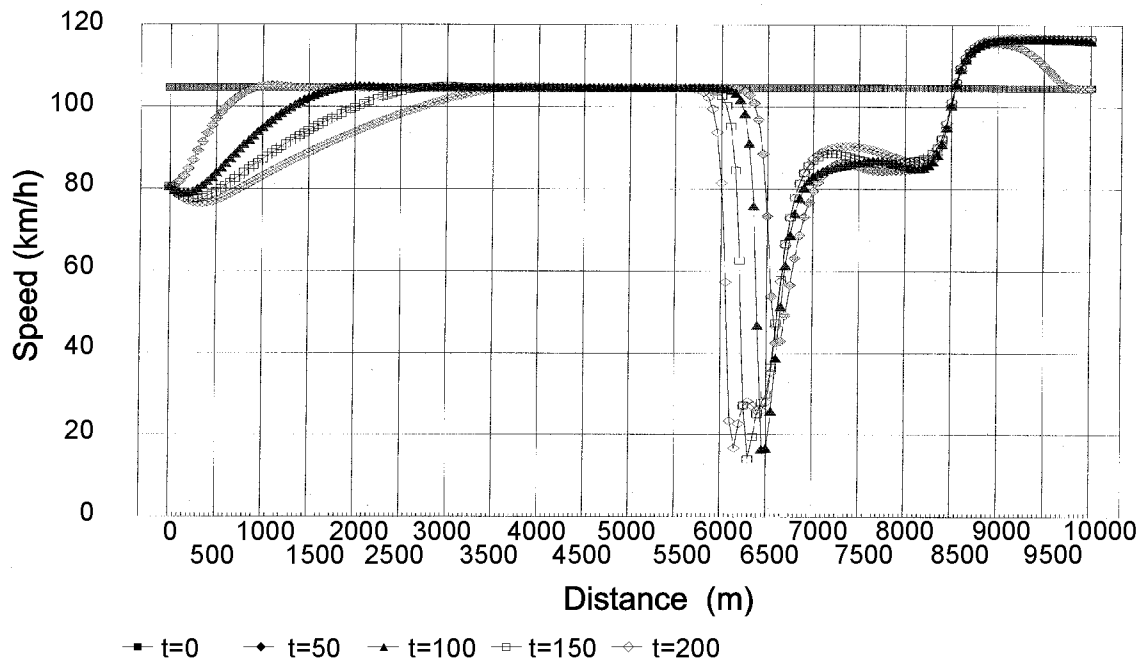

Figure 5.21b
Traffic Density Course after Six to Ten Minutes (derived from Sailer 1996).

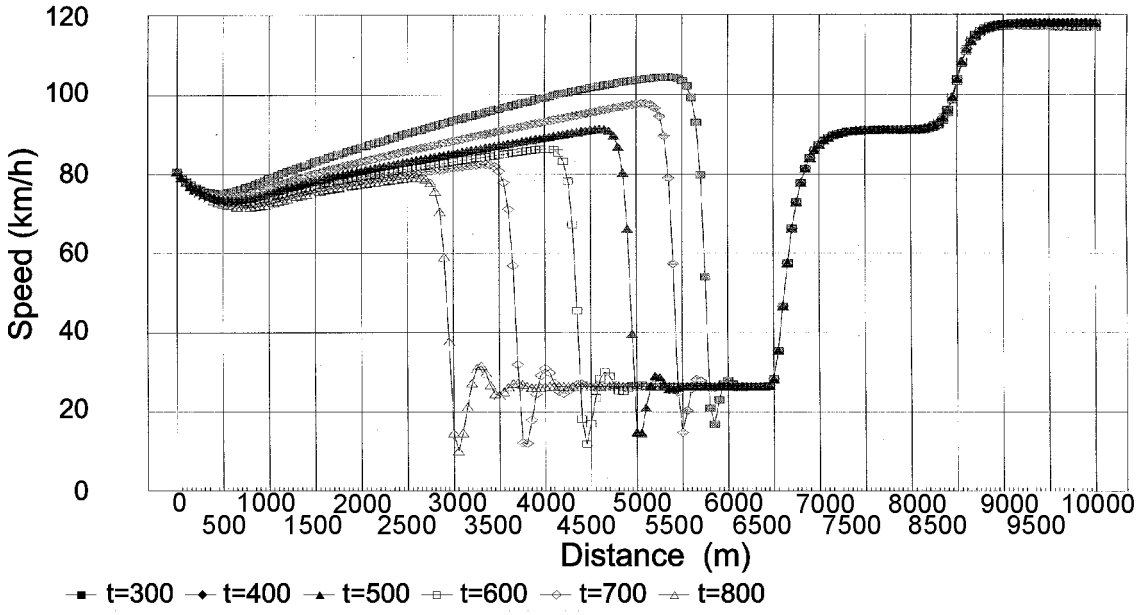

Figure 5.21c
Density Speed Course after 12 to 24 Minutes (derived from Sailer 1996).

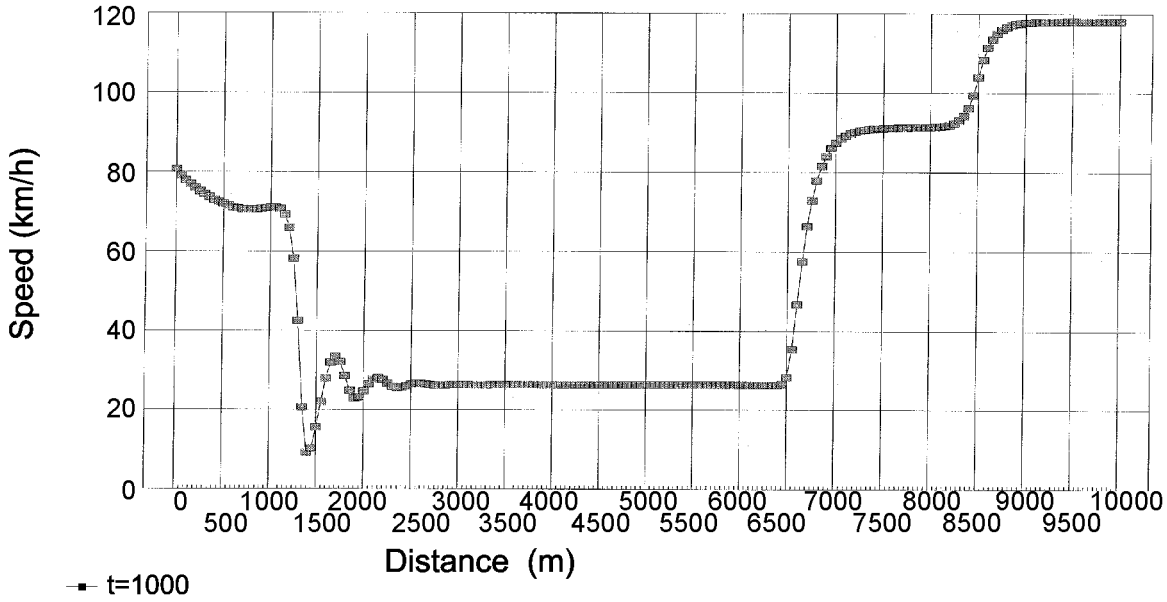

Figure 5.21d
Density Speed Course at the Bottleneck after 30 Minutes (derived from Sailer 1996).

hand and the fading of the overreaction regime border. It also shows that within the bottleneck additional small undulations occur - the annoying stop-start waves which characterize spilled-up traffic flow. The last snap shot gives an impression of the density distribution developing out of the initially constant distribution in the case of overcritical bottleneck density - keep in mind that the bottleneck itself lasts from 6.5 to 8.5 km. The stop-start waves lie in the congestion regime upstream of the lane reduction stretch.

5.2.9 Density Dependent Relaxation Time and Anticipation Coefficient

For simplicity up to now, a constant relaxation time τ with respect to density as well as a constant anticipation term has been regarded. Several attempts to describe both coefficients in a more realistic way have been undertaken. First, we look at the relaxation time with the dependencies (Michalopoulos et al. 1992):

$$\tau = \tau_0 \left(1 + r \frac{k}{k_{bump} - rk} \right) \quad 0 < r < 1 \tag{5.136}$$

Depending on the choice of r the relaxation time grows when traffic approaches density bumper to bumper and decreases when density is very low. The density dependence reflects the fact that approaching the desired speed seems almost impossible in dense traffic because of interactions with other drivers. This frustration effect gets smaller with decreasing density. In low dense traffic, a quiet relaxation to the original desired speed is possible which can be modelled by a smaller relaxation time (compare Figure 5.22). In Section 5.2.3 it was shown that the anticipation coefficient c_0^2 has the meaning of the standard deviation of the vehicular speed distribution. For this standard deviation, early measurements exist which show a broadening of the speed distribution for low dense traffic as a consequence of the possibility to realize individual desired speeds.

The narrowing of the speed distribution ends with beginning congestion. Stop-start waves and critical fluctuations which accompany unstable traffic flow lead to a broadening of the speed distribution. The reason is not due to different desired speeds but to the dynamics of traffic pattern formation which results in a broad speed distribution at a local measurement site (Heidemann 1986).

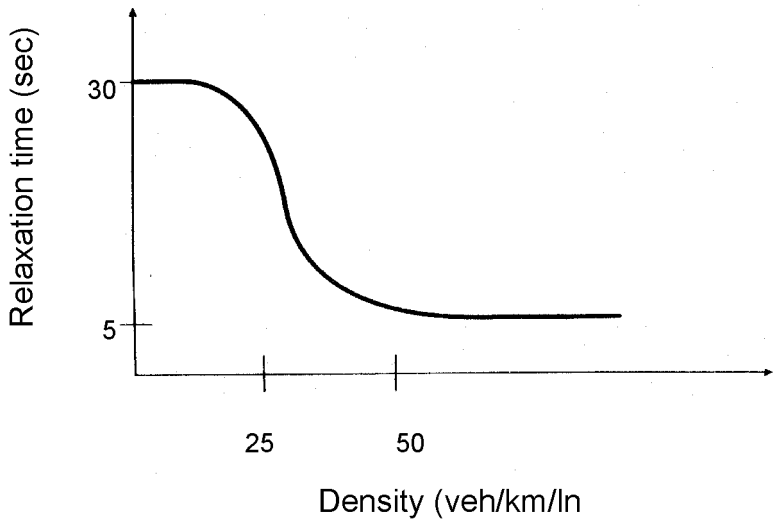

Note: Density-dependent relaxation time which reflects frustration effects in approaching the desired speed in dense traffic (Kühne and Langbein-Euchner 1993).

Figure 5.22
Density-Dependent Relaxation Time.

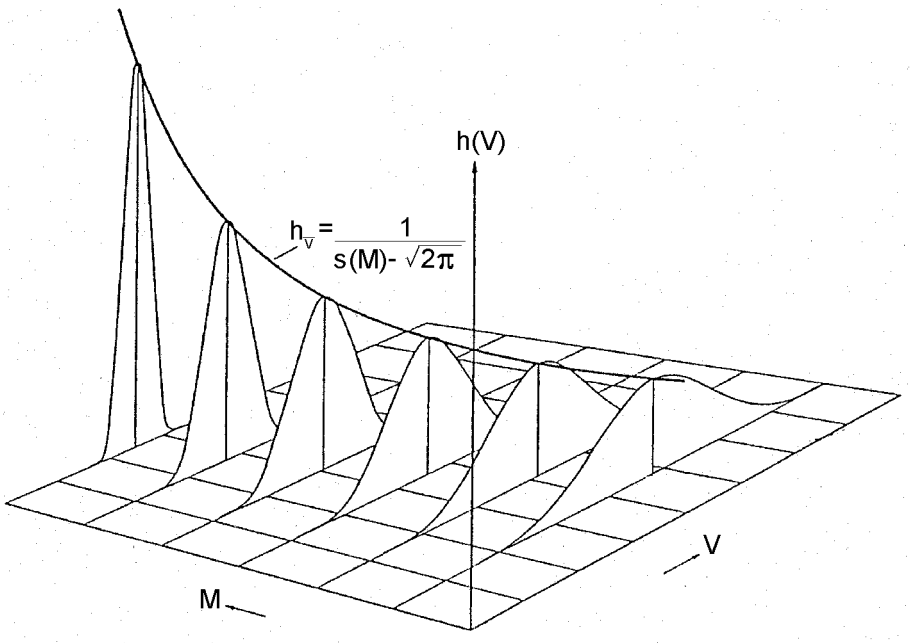

Figure 5.23
Speed Distribution Idealized Gaussian Distribution for Free and Nearly Free Traffic Flow (Pampel 1955).

Finally, in completely congested traffic, with creeping flow, mean speed and speed distribution coincide. There is no possibility for realization of different speeds. The standard deviation tends to zero. As a summary, Figure 5.24 shows the complete dependence of the anticipation coefficient c_o from density k. The estimation value stems from the validation calculations of Section 5.2.7.

In order to compare the numerical values with measurements of standard deviations from local speed distribution, consider that c_0^2 is equal to the momentary speed standard deviation and measurements result in local standard deviation values. The transformation succeeds with the relaxation (Leutzbach 1985),

$$\langle v_{loc} \rangle = \langle v_{mom} \rangle + \frac{\sigma_{mom}^2}{\langle v_{mom} \rangle} \quad , \langle ... \rangle = \textit{Expectation Value} \tag{5.137}$$

with σ_{loc}=18 km/h as a mean value for nearly free traffic flow, the transformation supports the assumption of c_0= 70km/h as a proper value in an overall constant approximation.

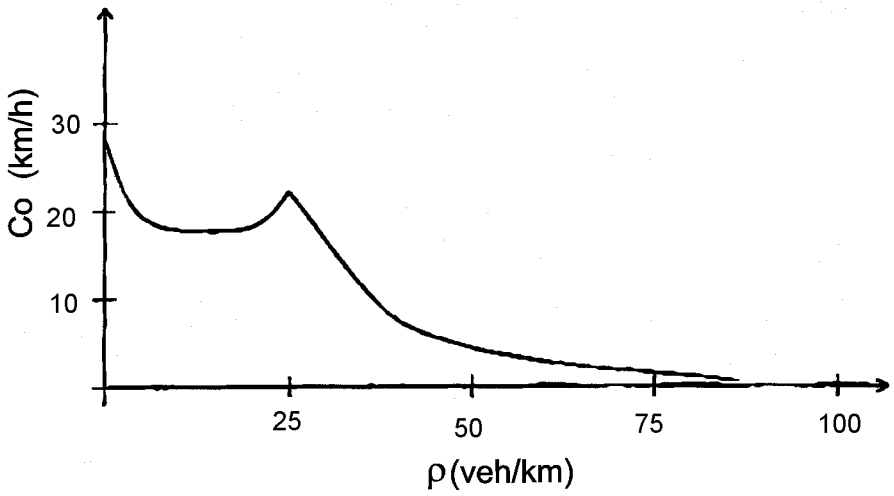

Figure 5.24
Anticipation Coefficient

5.3 Stochastic Continuum Models

5.3.1 Fluctuations in Traffic Flow

All measurements of speed, volume, and density indicate that traffic flow is a stochastic process which cannot be described completely by temporal and spatial development of macroscopic fluid variables. The question is how to incorporate the stochastic character into the macroscopic description and what consequences for early incident detection can be derived from the stochastic behavior with respect to time and space.

First, some measurements are reported which show speed distributions during jam formation and acceleration noise distributions. Measurements of traffic data which show the formation and dissolution of congestion are relatively scarce. As an example, measurements of traffic on Easter 1976 between 10:30 a.m. and 1:50 p.m. on the German Autobahn A5

Bruchsal-Karlsruhe as a two-lane highwayin each direction are presented. Figure 5.25 shows the mean speed time series as one-minute moving average with 30 sec offset for the passing lane in the direction of Karlsruhe at 617 km on April 15, 1976.

At time 4,600 sec, there is a speed breakdown which reoccurs after 10 minutes. In Figure 5.26 the corresponding speed distributions are recorded. Vehicle speeds are divided into groups of 5 km/h width. The frequency of vehicles in each speed class are determined during a 5-minute period with a beginning offset at the times 4,000 sec, 4,180 sec, 4,300 sec, 4,480 sec and 4,750 sec. The speed distribution beginning with 4,000 sec ends at 4,300 sec which is 5-minutes before the traffic breakdown. It shows an approximate Gaussian distribution with a standard deviation of 15 km/h and a near value of 120 km/h. Three minutes later, but still two minutes before the beginning of the congestion, there is a clear broadening of the distribution, traffic flow becomes more erratic; there is an increase in the number of both slower and faster cars. Five minutes later, the distribution lasts just until the beginning of the traffic breakdown - the speed distribution is even broader. Eight minutes later, the distribution is extremely broad since it includes non-stationary situations.

Finally, ten minutes later the distribution represents barely congested traffic with a relatively narrow distribution since critical fluctuations have dissolved.

5.3.2 Calculations of Speed Distributions

The broadening of the speed distribution when approaching the critical density connected with formation of jams and stop-start waves was theoretically found by Heidemann (1986). He calculated the speed distribution as a function of traffic density from transition probabilities between different speed classes. As critical density, a value of 25 veh/km is typical for traffic breakdowns due to overload.
To guarantee that the speed distribution is sufficiently updated and the regarded ensemble is stationary enough, the Sturges thumb rule (Sturges 1926) is applied for class width estimation.

In order to divide the speed distribution into a proper number of classes, an empirical rule is chosen that gives the class width:

$$\Delta u = \frac{u_{\max} - u_{\min}}{ld(2q_m t)} \tag{5.138}$$

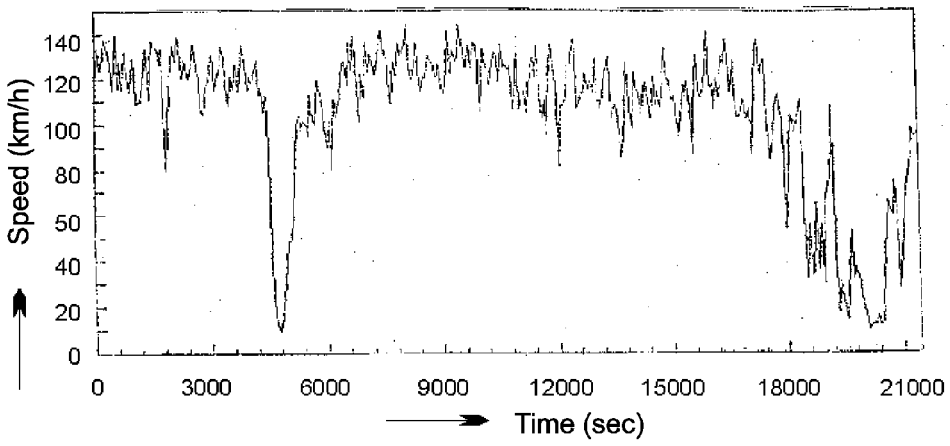

Figure 5.25
Time Series of Mean Speed on Autobahn A5 Bruchsal-Karlsruhe at 617 km, April 15, 1976, 10:30 a.m. - 1:50 p.m. (Leutzbach 1991).

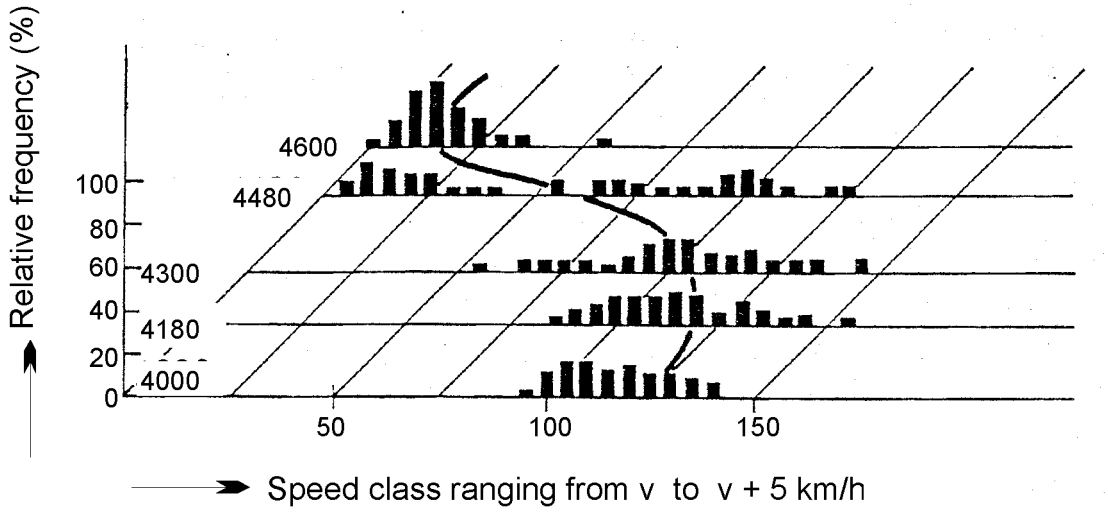

Figure 5.26
Speed Distribution During Congestion Formation of Figure 5.25.

where,

ld	=	logarithmus dualis
q_m	=	average volume
u_{max} - u_{min}	=	speed range
t	=	observation time

The meaning of this rule is that the proper speed class width is given by the range of speed values divided by the average information content of the corresponding measurement events. For a two-minute interval and an average traffic volume of 2,000 veh/h, the class width is

$$\Delta u = 10 \text{ km/h} \tag{5.139}$$

A finer subdivision would not make sense due to the strong fluctuations, and a coarser subdivision would unnecessarily blur details. The speed detection must, therefore, be done with errors less than 5 km/h which can be achieved by double inductive loops as well as millimeter-wave Doppler radar.

Within a macroscopic description of traffic flow, the incorporation of fluctuation is possible in two ways. First, a noise term can be added to the acceleration equation. The model equations are then rewritten to include a fluctuating force, Γ,

$$\begin{aligned} k_t + (ku)_x &= 0 \\ u_t + uu_x &= \frac{1}{\tau}\left(U_e(k) - u\right) - c_0^2 \frac{k_x}{k} + \frac{\mu_0}{k} u_{xx} + \Gamma \end{aligned} \tag{5.140}$$

This addition has the effect that speed and density no longer take exact values but are randomly distributed around a mean value instead. The fluctuation term describes noise by an all-in-one representation of random influences such as bumps, irregularities in street guidance, and fluctuations in drivers´ attention. The noise due to discrete character of the measurement events is superposed and can be included in the fluctuating force description. In the simplest case, the stochastic quantity Γ is δ - correlated in space and time with a Gaussian distributed while noise spectrum

$$\begin{aligned} &< \Gamma(x,t) > = 0 \\ &< \Gamma(x,t)\ \Gamma(x',t') > = 2\ \sigma_0^2\ c_0 (x - x')\ \delta(t - t') \end{aligned} \tag{5.141}$$

where <.....> denotes the expectation value over an ensemble of realizations. The quantity σ_0 is the standard deviation of the speed distribution for free traffic flow. The δ - correlation means that correlations decay rapidly in space and time at least within the space scale $c_o\tau$ (= 35 m) and within the time scale τ (=1.8 sec).

Another approach in a macroscopic stochastic description considers the convection nonlinearities as feedback effects. These effects lead to a competition between saturation of strong spatial variations and over-proportional amplification of slow undulations.

The effect can be explained by the marginally stable solution (compare the linear stability analysis of Section 5.2.5). Introducing the state vector η which summarizes density and speed with respect to an operating point $k_0 \mid U_e(k_0)$ in a slightly different way as in Section 5.2.6

$$\eta = \begin{pmatrix} \tilde{k} = ln\frac{k}{k_0} \\ \tilde{u} = \frac{u - u_e(k_0)}{c_0} \end{pmatrix} \tag{5.142}$$

the basic equations read in a comprehensive form

$$\eta_{t'} + \tilde{u}\eta_{x'} = -L\eta \qquad L = \begin{pmatrix} 0 & \partial_{x'} \\ a+1+\partial_{x'} & 1-\nu\partial_{x'}^2 \end{pmatrix} \tag{5.143}$$

with

$$x' = \frac{x - U_e(k_0)t}{c_0\tau} \qquad t' = \frac{t}{\tau} \tag{5.144}$$

as independent variables and the approximations

$$\frac{1}{c_0}U_e(k) \approx \frac{1}{c_0}U_e(k_0) - (a+1)\tilde{k}$$
$$\nu = \frac{\mu}{kc_0^2\tau} \approx constant \tag{5.145}$$

At the marginal stable point (~ suppressed)

$$k = -u \tag{5.146}$$

is fulfilled and the linear part in the basic equations approximately vanishes. The marginally stable solution then obeys the equation (' suppressed)

$$u_t + uu_x = 0 \tag{5.147}$$

which has the solution

$$u = f(x - u\,t) \tag{5.148}$$

for the initial condition $u\ (x,\ t = 0) = f\ (x)$. The solution u is dependent on u itself. This is a typical feedback with foundation in the convection nonlinearity $u\ u_x$. The feedback affects saturation in the case of strong spatial variations (uniform steeping) and over-proportional amplification of slow spatial variations (amplification of small disturbances). The competition between these effects produces irregularities near the stability threshold. These nonlinearity fluctuations describe deterministic motion and do not need noise for explaining an erratic behavior. It superposes the omnipresent noisy oscillations and can be used separately for representation of fluctuations in traffic flow.

5.3.3 Acceleration Noise

A stochastic continuum theory must be able to quantify the noisy character of traffic flow due to individually different accelerations of the vehicles which build up a regarded ensemble. The drivers of such an ensemble are influenced by many disturbances like bumps, curves, lapses of attention, and different engine capabilities. The acceleration of a regarded vehicle can be split into a term which describes velocity control within a car following model and a random term which is the natural acceleration noise. This noise is usually defined as the root mean square deviation of the acceleration of the vehicle driven independently of other vehicles (Herman et al. 1959). Besides the dependence on the type of road, the number of curves, and the occurrence of bottlenecks in traffic, the acceleration noise is a function of the density and traffic volume.

First tests to determine the noise distributions experimentally are reported in Herman et al. 1959. An accelerometer of an equipped test car was evaluated for trips under different density conditions and with different driving tasks for the driver. When one merely tries to keep up with the stream, the distribution is essentially Gaussian with a standard deviation of $\sigma = 0.03g$, while the distribution ranges from - 0.05g to

+ 0.05g. When the driver is to attempt 8 to 16 km/h faster than the stream average, high accelerations and decelerations occur more frequently giving rise to two wings and a significant broadening (σ = 0.07g) of the distribution.

The acceleration noise as a measure of the acceleration distribution shows similar behavior compared to the speed distribution. A measurement series described by Winzer (1980) is reported, which has investigated the trip recorders of a vehicle fleet floating in the traffic flow on the Autobahn A5 Durlach-Bruchsal, Germany. One hundred sixty measurement trips were evaluated. All possible traffic flow situations were encountered although free or nearly free traffic flow made up the majority. Figure 5.27 shows the results of standard deviation of the acceleration noise for different traffic densities. A singularity of the standard deviation, of the acceleration noise distribution, occurs in the vicinity of the critical density which shows that the broadening of the speed distribution coincides with the broadening of the acceleration noise distribution as an expression for traffic becoming erratic with critical fluctuations in the transition regime between stable and unstable traffic flow. These observations fit with early investigations of Herman et al. (1959) and Drew et al. (1965) who, for the first time, looked at acceleration noise distributions.

After quantifying the experimental situation a continuum theory approach is sketched. As the boundary and initial conditions are essential and, for reasons of clarity, periodic boundary conditions will be considered.

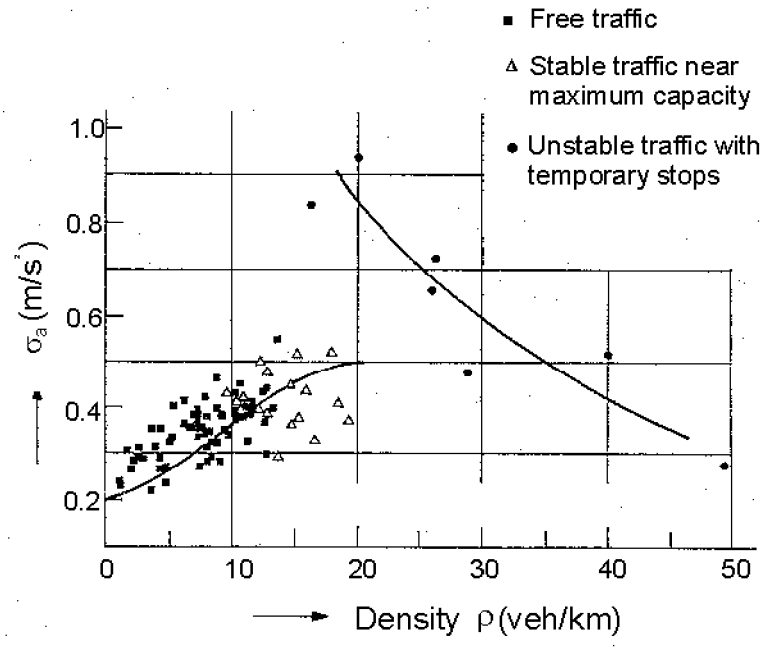

Note: Data from an evaluation of 160 trips on the Autobahn A5 between exit Durlach and exit Bruchsal near Karlsruhe, Germany.

Figure 5.27
Standard Deviation of the Acceleration Noise for Different Traffic Densities (Winzer 1980).

These conditions claim

$$q(0.t) = q(L.t)$$
$$u(0.t) = u(L.t) \qquad u_x(0.t) = u_x(L.t) \tag{5.149}$$

where L is the length of the regarded periodic interval. The periodic boundary conditions seem somewhat artificial, but they are easy to handle. In the case for $L \to \infty$ an independence of specific boundary conditions can be shown (Kerner and Konhäuser 1993b). As carried out in Kerner and Konhäuser (1993b), the initially fixed number of vehicles remains constant:

$$N = \int_0^L k(x.t)dx = k_{hom}\, L = constant \tag{5.150}$$

with k_{hom} the vehicle density in homogeneous flow. The corresponding value of the homogeneous speed is deduced from the equilibrium speed density relation

$$u_{hom} = U_e(k_{hom}) \tag{5.151}$$

if N and L are given, there is only one homogeneous state

$$k = k_{hom} \qquad u = u_{hom} \tag{5.152}$$

this has a consequence that a Fourier series for an arbitrary solution has to exclude the wave number l = 0 and reads

$$k(x.t) = k_{hom} + \sum_{n\neq 0} k_n e^{il_n x+\omega(l_n)t} l_n = \frac{2\pi n}{L} n = \pm 1_1 \pm 2_1 ... \tag{5.153}$$

$$u(x.t) = U_e(k_{hom}) + \sum_{n\neq 0} u_n e^{il_n x+\omega(l_n)t}$$

The lowest wave number $l_1 = \frac{2\pi}{L}$ determines the stability range which reads (Kühne and Beckschulte 1993)

$$\nu l_1^2 < a$$

with

$$a = -1 - \frac{k_{hom}}{c_0} U_e'(k_{hom}) \qquad \nu = \frac{\mu_0}{k_{hom}^2 c_0^2 t} \tag{5.154}$$

For simplification, further stationary solutions of the underlying traffic flow model are regarded. In order to obtain stationary solutions, the collective variable

$$z = x - u_g t \tag{5.155}$$

is introduced as the only independent variable. The equation of continuity can be integrated

$$k(z) = \frac{Q_0}{u(z) - u_g} \tag{5.156}$$

where the external given flow Q_0 is linked to the solid vehicle number N by

$$N = \int_0^L k(z)\ dz = Q_0 \int_0^L \frac{dz}{u(z) - u_g} \tag{5.157}$$

The stationary profile equation has the form of a non-linear Newton equation of motion

$$\mu u_{zz} + Q_0 \left(\frac{1}{(u-u_g)^2} - 1 \right) u_z + \frac{Q_0}{u-u_g} \left(\frac{1}{c_0} u_e\left(\frac{Q_0}{u-u_g} \right) - u \right) = 0 \tag{5.158}$$

5.3.4 Microscopic Time Gap Distribution and Macroscopic Traffic Volume Distribution

The basis of a stochastic description of traffic flow is that speed and density do not adopt discrete values but instead are randomly distributed around a mean value. The microscopic behavior is no longer given by a fixed distance law, but by a time gap distribution as the macroscopic description is stated by a probability distribution for the traffic volume.

The connection between microscopic time gap distribution and macroscopic traffic volume distribution is explained by means of elementary considerations:

If $p(n,s)$ = probability of finding n vehicles during the times

and $q\ ds$ = arrival probability of one vehicle during the infinitesimal time ds when q is the actual stationary traffic volume.

$1\text{-}q\ ds$ = probability that the vehicle number remains unchanged during the time ds,

then the probability of finding n vehicles during the time $s+ds$ is

$$p(n, s+ds) = p(n-1, s)qds + p(n, s)(1-qds) \quad (5.159)$$

Since the vehicle number n can be generated by an arrival during the time extension between s and $s+ds$ starting from $n-1$ vehicles with one additional arriving or by a conservation of the vehicle number n. Expanding with respect to ds gives

$$\frac{\partial p(n, s)}{\partial s} = \frac{(qs)^n}{u!} e^{-qs} \quad (5.160)$$

for the actual traffic volume q. If the traffic volume itself is distributed with a distribution $W(q)$ one has to integrate overall possible values q

$$p(n, s) = \int_0^\infty \frac{(qs)^n}{n!} e^{-qs} W(q)dq \quad (5.161)$$

from which the time gap distribution,

$$p(o, s) \equiv P(t_{gap} \geq s) = \int_0^\infty e^{-qs} W(q)dq \quad (5.162)$$

can be derived. This probability is identical with the probability that the time gap between the arrival of the next vehicle is larger than s. Time gap distribution (compare Figure 5.28) and traffic volume distribution are therefore related by Laplace transformation.

For practical reasons, the empirical data are approximated with a least square fit as Padé-expansion

$$P(s) = \frac{1 + a, s}{1 + b, s + b_2 s^2} \quad (5.163)$$

It should be noted that for $s \leq 0.2$ sec, the probability $P(s)$ has constantly the value one. This refers to a minimum time gap during which certainly no vehicle is registered and which is caused by the finite length of the vehicles.

Figure 5.29 reports the corresponding Laplace transformation as the traffic volume distribution (Kühne 1989). The maximum of the traffic volume distribution changes from $q = 0$ to $q \neq 0$ at a

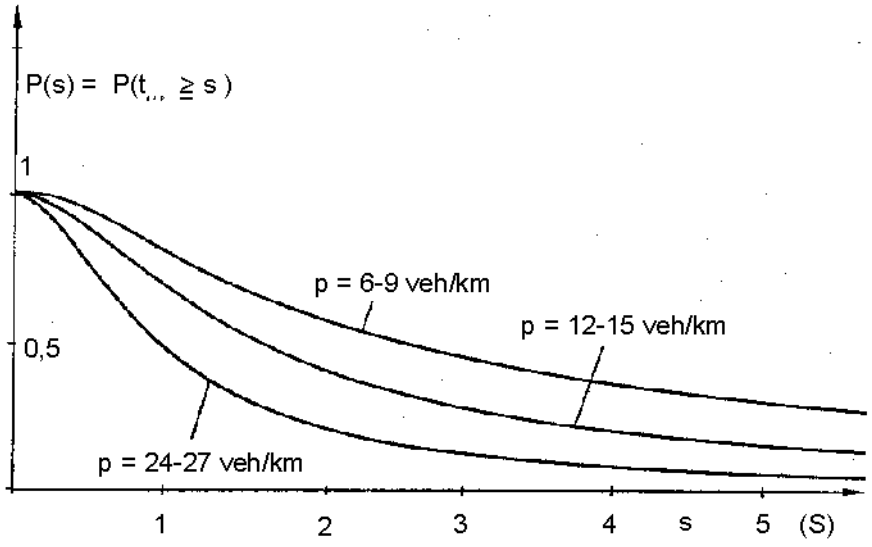

Figure 5.28
Time Gap Distribution for the Median Lane
From the Autobahn A8 near Stuttgart, Germany.

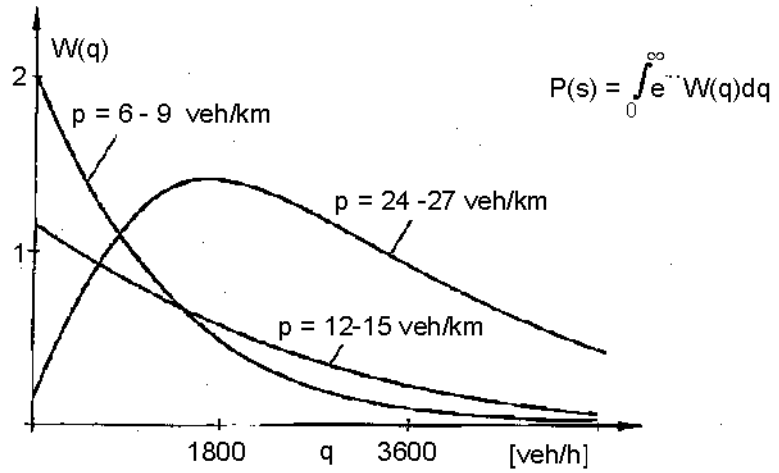

Figure 5.29
Traffic Volume Distribution as Result of a Laplace Transformation.

critical density value of about 25 veh/km/lane. The change in the shape of value of the traffic volume distribution occurs at the same critical traffic density for which homogeneous traffic flow becomes unstable. This coincidence expresses the connection between microscopic time gap distribution and macroscopic instability phenomena.

The maximum of the traffic volume distribution is not identical with the mean value which is given by

$$\bar{q} = \int_0^\infty qW(q)dq \tag{5.164}$$

It is just the most likely value in case of a measurement series covering all possible traffic volume values!

References

Ansorge, R. (1990). *What does the Entropy Condition Mean in Traffic Flow Theory?* Transportation Research, 24 B, pp. 133-144.

Babcock, P. S. et al. (1982). *Freeway Simulation and Control*. University of California at Berkeley, Institute of Transportation Studies, UCB-ITS, RR 82-13.

Bui, D. D., P. Nelson, and S. L. Narasimhan (1992) *Computational Realization of the Entropy Condition in Modelling Congested Traffic Flow*. Res. Rep., 1232-7, Texas Transporation Institute, Texas A & M University, College Station, TX.

Castillo, J. M., P. Pintado, and F. G. Benitez (1993). *A Formulation for the Reaction Time of Traffic Flow Models.* In C. Daganzo (ed). Theory of Transportation and Traffic Flow.

Cremer, M. (1979). *Der Verkehrsfluß auf Schnellstraßen (Traffic Flow on Freeways)*. Springer, Berlin.

Cremer, M. and A. D. May (1985). *An Extended Traffic Model for Freeway Control.* University of California at Berkeley, Institute of Transportation Studies, Research Report, UCB-ITS, RR 85-7.

Cremer, M., F. Meißner, and S. Schrieber (1993). *On Predictive Schemes in Dynamic Rerouting Strategies.* In C. Daganzo (ed). Theory of Transportation and Traffic Flow, pp. 407-462.

Dressler, R. F. (1949). *Mathematical Solution of the Problem of Roll-Waves in Inclined Open Channels*. Commun. Pure and Appl. Math, 2, pp. 149-194.

Ferrari, P. (1989). *The Effect of Driver Behaviour on Motorway Reliability*. Transportation Research, 23B, pp. 139-150.

Gazis, D. C., R. Herman, and G. H. Weiss (1962). *Density Oscillations Between Lanes of a Multilane Highway*. Oper. Res., 10, pp. 658-667.

Gerlough, D. L. and M. J. Huber (1975). *Traffic Flow Theory: A Monograph*. Transportation Research Board, S.R.165.

Greenshields, B. D. (1934). *A Study of Traffic Capacity.* HRB Proc., Vol. 14, pp. 448-477.

Hauer, E. and V. F. Hurdle (1979). *FREFLO: Discussion of the Freeway Traffic Model.* Transportation Research Record, 722, pp. 75-77.

Helbing, D. (1994). *An Improved Fluid-Dynamic Model for Vehicular Traffic*. Phys. Rev. E. (to be published).

Heidemann, D. (1986). *An Analytic Calculation Method for Speed Distribution in Dependence on Traffic Density.* Z. für Verkehrswiss. (Traffic Engineering), pp. 57-68.

Heidemann, D. (1986). *Eine analytische Berechnungsmethode für Geschwindigkeitsverteilungen in Abhängigkeit von der Vekehrsdichte (An Analytical Calculation Method for Speed Distributions in Dependence of Traffic Density).* Zeitschrift für Verkehrswesenschaft (Journal of Transportation Science). Verkehrs Verlag Pub., Düsseldorf, pp. 57-68.

Hermann, R. et al. (1959). *Traffic Dynamics: Analysis of Stability in Car Following*. Op. Res., 7, pp. 86-106.

Kerner, B. S. and P. Konhäuser (1993a). *Makroskopische Verkehrssimulation - Einsatzmöglichkeiten und numerisches Lösungsverfahren (Macroscopic Traffic Simulation - Applications and Numerical Solution Method) in: K.H. Münch (ed).* Simulation of Traffic Systems - Working Group on Simulation in connection with the 8th Symposium on Simulation Techniques, Berlin, 1993, Vieweg Pub., pp. 105-130.

Kerner, B. S. and P. Konhäuser (1993b). *Cluster Effect in Initially Homogeneous Traffic Flow.* Phys. Rev. E. 48, Oct 1993, pp. 2335-2338.

Koshi, M., M. Iwasaki, and I. Ohkwa (1981). *Some Findings and an Overview on Vehicular Flow Characteristics.* In V. F. Hurdle, E. Hauer, G. N. Stewart (edts.). Proceedings of the 8th International Symposium on Transportation and Traffic Theory, Toronto, pp. 295-306.

Kühne, R. D. (1984). *Macroscopic Freeway Model for Dense Traffic* in N. Vollmuller (ed). 9th Int'l Symposium on Transportation and Traffic Theory: VNU Science Press, pp. 21-42.

Kühne, R. D. (1987). *Freeway Speed Distribution and Acceleration Noise* in N. H. Gartner, N. H. M. Wilson (edts.). Proceedings of the Tenth International Symposium on Transportation and Traffic Theory, Elsevier, pp. 119-137.

Kühne, R. D. (1989). *Microscopic Distance Strategies and Macroscopic Traffic Flow Models.* Proceedings of the CCCT '89, Paris, pp. 267-272.

Kühne, R. D. (1991). *Traffic Patterns in Unstable Traffic Flow on Freeways.* In U. Brannolte (ed). Highway Capacity and Level Service, Balkema Rotterdam, pp. 211-223.

Kühne, R. D. and K. Langbein-Euchner (1995). *Parameter Validation.* Report as an Order of Daimler-Benz Research, Stuttgart. Available by *Steierwald Schönharting und Partner*, Stuttgart.

Kühne, R. D. and R. Beckschulte (1993). *Non-linearity Stochastics of Unstable Traffic Flow,* Proceedings of the 12th Int'l Symposium on the Theory of Traffic Flow and Transportation, C. F. Daganzo (ed.). Berkeley, CA, pp. 367-386.

Leutzbach, W. (1985). *Introduction to the Theory of Traffic Flow*. Springer Pub., pp. 184-193.

Leutzbach, W. (1991). *Measurements of Mean Speed Time Series Autobahn A5 near Karlsruhe, Germany.* Institute of Transport Studies, University of Karlsruhe, Germany.

Leutzbach, W. (1991). *Measurements of Mean Speed Time Series Autobahn A5 near Karlsruhe, Germany.* Institute of Transport Studies, University of Karlsruhe, Germany.

Lighthill, M. H. and G. B. Whitham, (1955). *On Kinematic Waves-II. A Theory of Traffic Flow on Long Crowded Roads.* Proceedings, Royal Society (London), A229, No. 1178, pp. 317-345.

McCrank, J. (1993). *Measurement Data Interstate 80 Oakland, San Jose* within the Freeway Service Patrol Evaluation Project, Department of Transportation District IV, Oakland, CA.

Michalopoulos, P. G. (1988). *Analysis of Traffic Flow at Complex Congested Arterials.* Transportation Research Record, 1194, pp. 77-86.

Michalopoulos, P. G., D. E. Beskos, and Y. Yamauchi, (1984). *Multilane Traffic Flow Dynamics: Some Macroscopic Considerations.* Transportation Research, 18B, No. 4/5, pp. 377-395.

Michalopoulos, P. G., E. Kwon, and E. G. Khang, (1991). *Enhancements and Field Testing of a Dynamic Simulation Program.* Transportation Research Record, 1320, pp. 203-215.

Michalopoulos, P. G., Jaw Kuan Lin, and D. E. Beskos, (1987). *Integrated Modelling and Numerical Treatment of Freeway Flow.* Appl. Mathem. Model, Vol. 11, No. 401, pp. 447-458.

Michalopoulos, P. G. and V. B. Pisharody (1980). *Platoon Dynamics on Signal Controlled Arterials.* Transportation Science, Vol. 14, No. 4, pp. 365-396.

Michalopoulos, P. G. and V. Pisharody (1981). *Derivation of Delays Based on Improved Macroscopic Traffic Models*. Transportation Research Journal, 15B, No. 5, pp. 299-317.

Michalopoulos, P. G., G. Stephanopoulos, and V. B. Pisharody (1980). *Modelling of Traffic Flow at Signalized Links.* Transportation Science, Vol. 14, No. 1, pp. 9-41.

Michalopoulos, P. M., P. Yi, and A. S. Lyrintzis (1992). *Development of an Improved High-Order Continuum Traffic Flow Model.* Transportation Research Record, B65, pp. 125-132.

Müller-Krumbhaar, H. and J. P. Eerden v.d. (1987). *Some Properties of Simple Recursive Differential Equations*. Z. Physics B - Condensed Matter 67, pp. 239-242.

Pampel, F. (1955). *Ein Beitrag zur Berechnung der Leistungsfähigkeit von Straßen (A Contribution for Calculating the Capacity of Roads).* Forschungsgesellschft für das Straßenwesen, Köln (Road Transport Research Society, Cologne), Vol. 15, Kirschbaum Pub., pp. 3-30.

Papageorgiou, M., J. M. Blosseville, and H. S. Habib (1989). *Macroscopic Modelling of Traffic Flow on Boulevard Périphérique*. Transportation Research Board, 23B, pp. 29-47.

Papageorgiou, M., J. M. Blosseville, and H. Hadj-Salem (1990). *Modelling and Real-Time Control of Traffic Flow on the Southern Part of the Boulevard Peripherique in Paris Part I: Modelling, Part II: Coordinated Ramp Metering.* Transportation Research A, 24A, pp. 345-370.

Payne, H. J. (1979). *FREFLO: A Macroscopic Simulation Model of Freeway Traffic.* Transportation Research Record 722, pp. 68-77.

Phillips, W. F. and F. Prigogine (1979). in N. Lampis (ed): Proc. of the 1978 IEEE Conf. on Decision and Control including the 17th Symposium on Adaptive Processes, San Diego, CA, pp. 1032-1036.

Prigogine, I. and R. Herman (1991). *Kinematic Theory of Vehicular Traffic*. Am. Elsevier Publ., New York.

Richards, P. I. (1956). *Shock Waves on the Highway.* Oper. Res., 4 (1), pp. 42-51.

Sailer, H. (1996). *Fuid Dynamical Modelling of Traffic Flow on Highways - Physical Basis and Numerical Examples*; Dissertation. (submitted for a Diploma) at the Institute for Theoretical Physics, University Innsbruck.

Stephanopoulos, G. and P. G. Michalopoulos (1979). *Modelling and Analysis of Traffic Queue Dynamics at Signalized Intersections.* Transportation Research, Vol. 13A, pp. 295-307.

Stephanopoulos, G. and P. G. Michalopoulos (1981). *An Application of Shock Wave Theory to Traffic Signal Control.* Transportation Research Journal, Vol. 5B, pp. 35-51.

Sturges, H. A. (1926). *The Choice of a Class Interval.* J. Am. Statist. Assoc., pp. 65-66.

Treiterer, J. (1973). *Traffic Control Characteristics of Urban Freeways.* Proceedings of the International Road Federation World Meeting, Munich.

Treiterer, J. and J. A. Myers (1974). *The Hysteresis Phenomena in Traffic Flow.* 6th Int'l. Symposium on Transportation and Traffic Theory, Reed Pty Ltd., Artamon N.S.W., pp. 13-38.

Varaija, P. P., et al. (1994). *Freeway Service Patrol Evaluation Project*. University of California at Berkeley, PATH MOM-91, Progress Report.

Verweij, H. D. (1985). *Filewaarschuwing en Verkeer-safwikkeling*. Ministry of Traffic and Water- Ways, Delft, The Netherlands.

Wemple, E. A., A. M. Morris, and A. D. May (1991). *Freeway Capacity and Flow Relationships* in: U. Brannolte (ed). Highway Capacity and Level of Service, Balkema Pub., pp. 439-456.

Whitham, G. B. (1974). *Linear and Nonlinear Waves.* Wiley & Sons, NY, pp. 68-95.

Winzer, Th. (1980). *Messung von Beschleunigungsverteil-ungen (Measurements of Acceleration Distributions) Forschung Straßenbau und Straßenverkehrstechnik (Research on Road Construction and Traffic Engineering).* Federal Ministry of Transportation, Bonn, Germany (ed.), Vol. 319, 1980.